PHILOSOPHICAL TRANSACTIONS OF THE ROYAL SOCIETY B BIOLOGICAL SCIENCES

Cyclic AMP Oscillations in Suspensions of Dictyostelium discoideum

P. B. Monk and H. G. Othmer

Phil. Trans. R. Soc. Lond. B 1989 **323**, 185-224
doi: 10.1098/rstb.1989.0005

Phil. Trans. R. Soc. Lond. B **323**, 185–224 (1989) [185]
Printed in Great Britain

CYCLIC AMP OSCILLATIONS IN SUSPENSIONS OF *DICTYOSTELIUM DISCOIDEUM*

By P. B. MONK[1] and H. G. OTHMER[2]

[1] *Department of Mathematics, University of Delaware, Newark, Delaware* 19716, *U.S.A.*
[2] *Department of Mathematics, University of Utah, Salt Lake City, Utah* 84112, *U.S.A.*

(*Communicated by J. D. Murray, F.R.S. – Received* 27 *October* 1987)

CONTENTS

A model developed previously for signal relay and adaptation in the cellular slime mould *Dictyostelium discoideum* is shown to account for the observed oscillations of calcium and cyclic AMP in cellular suspensions. A qualitative argument is given which explains how the oscillations arise, and numerical computations show how characteristics such as the period and amplitude of the periodic solutions depend on

parameters in the model. Several extensions of the basic model are investigated, including the effect of cell aggregation and the effect of time delays in the activation and adaptation processes. The dynamics of mixed cell populations in which only a small fraction of the cells are capable of autonomous oscillation are also studied.

1. Introduction

The cellular slime mould *Dictyostelium discoideum* is an important system for the study of many developmental processes, including intercellular communication, chemotaxis and differentiation. In a favourable environment the free-ranging individual amoebae feed on bacteria and divide by binary fission, but if the food supply is exhausted an elaborate developmental programme is initiated. After a period of starvation the cells attain relay competence and can respond to an external cyclic AMP signal by synthesizing and releasing cyclic AMP. This is called the relay response. The fraction of relay competent cells in a population increases with time after starvation, and at 10 h post starvation almost all cells are relay competent (Gingle & Robertson 1976). At about 8 h post-starvation the cells begin aggregating in response to periodic waves of cyclic AMP initiated by randomly located pacemaker cells. The proportion of autonomously signalling cells in an aggregation field rises from zero at about 7 h post starvation and saturates at a small fraction of the total population within 21 h (Raman *et al.* 1976). At the end of aggregation the cells form a cylindrical slug or grex which may migrate on the substrate for some time. After migration the slug forms a fruiting body, which consists of an erect stalk that supports a spherical cap containing spores. Under favourable conditions of temperature and humidity the spores are released and can germinate, and the cycle begins anew (Bonner 1967).

A model for cyclic AMP synthesis and signal transduction in relay competent cells has been proposed and investigated in two previous papers (Rapp *et al.* 1985*a*; Othmer *et al.* 1985), hereafter referred to as (I) and (II), respectively. One special case of this model is applicable to the experimental protocol of Devreotes and co-workers (Devreotes *et al.* 1979; Devreotes & Steck 1979; Dinauer *et al.* 1980*a–c*). Here relay-competent cells are stimulated by a specified temporal sequence of extracellular cyclic AMP concentrations in a perfusion apparatus, and the resulting response of secreted cyclic AMP is measured. The experiments show that the concentration of intracellular cyclic AMP and the rate of cyclic AMP secretion adapt to constant levels of extracellular cyclic AMP. In this context adaptation means that a step change from one constant level of the extracellular concentration of cyclic AMP to a higher constant level causes a transient increase in the rate of cyclic AMP synthesis and secretion, followed by a return to basal levels. The relay response is not an all-or-nothing phenomenon, because adaptation to one concentration of cyclic AMP does not preclude a response to further increases in cyclic AMP. Moreover, adaptation is seldom perfect, in that the secretion rate does not return to precisely the basal level after stimulation, but perfect adaptation can be used as a standard when evaluating models.

A cyclic AMP stimulus also initiates a chemotactic response that peaks before the maximal relay response. This response includes changes related to movement (Newell 1986), and the transient production of cyclic GMP, which peaks about 5 s after stimulus (Wurster & Butz 1983). The chemotactic response, which is apparently independent of the relay–adaptation response (Brenner & Thomas 1984), will be treated in a later paper.

The model developed in (I) and (II) is based on the assumption that calcium inhibits adenylate cyclase directly, or indirectly via a calcium-activated process such as phos-

PHILOSOPHICAL TRANSACTIONS OF THE ROYAL SOCIETY B BIOLOGICAL SCIENCES

phorylation, as it does in other cells (cf. (I) and §6 for references to the experimental literature). This inhibition produces adaptation as follows. Following an increase in the extracellular cyclic AMP concentration, the fraction of cell-surface receptors bound with cyclic AMP increases and more adenylate cyclase is activated, which leads to an increase in the intracellular cyclic AMP concentration and the cyclic AMP secretion rate. The external cyclic AMP stimulus also triggers an influx of calcium, and the increase of intracellular calcium following stimulation reduces the rate of cyclic AMP production. As we showed in (II), if the sensitivity of the enzyme to activation and inhibition is adjusted correctly, the intracellular cyclic AMP concentration and secretion rate return to their basal levels following a step increase in external cyclic AMP. Thus adaptation of the intracellular cyclic AMP level and the secretion rate results from an increase in the intracellular calcium concentration, which does not exhibit adaptation. The results in (II) and those given later in this paper show that this model reproduces the results obtained in the perfusion experiments well.

Experimental results on the dynamics of cellular suspensions provide data for further tests of the model. Experiments using suspensions differ from perfusion experiments because the extracellular calcium and cyclic AMP concentrations are not clamped, and thus self-stimulation of the cells can occur. If aggregation-competent cells are suspended in buffer and agitated, a series of spikes followed by sinusoidal oscillations in the light-scattering properties of the suspension are observed (Gerisch & Hess 1974). Measurements of the intra- and extracellular cyclic AMP concentration show that the oscillations in light scattering are correlated with oscillations in both cyclic AMP levels (Gerisch *et al.* 1979). The amplitude of the intracellular cyclic AMP oscillation typically ranges between 7 and 20 μM, with a minimum concentration of about 3 μM (Gerisch & Wick 1975; Brenner 1978). The amplitude of the oscillation in extracellular cyclic AMP is approximately 2 μM (Gerisch *et al.* 1975; Gerisch & Wick 1975; Brenner 1978), and the period is approximately 5–10 min when the cell density is in the range of 10^7 to 2×10^8 cells cm^{-3} (Gerisch & Hess 1974; Gerisch & Wick 1975; Gerisch *et al.* 1975; Weijer *et al.* 1984; Gottmann & Weijer 1986). Gerisch & Hess (1974) report that the addition of cyclic AMP to the suspension causes phase shifts and even temporary extinction of the oscillatory light scattering response. Furthermore, if cyclic AMP is added to the suspension at a sufficiently high rate the oscillations are suppressed completely. The suppression of oscillations under maintained extracellular concentrations of cyclic AMP is consistent with the observations of Devreotes *et al.* discussed previously, because the two experimental configurations are essentially the same in this case.

Because calcium is one of the major components in our model, data on the temporal variations of extracellular calcium in suspensions provides another means of testing the model. The variations in extracellular calcium and the calcium influx into the cells in suspension experiments have been studied in (Malchow *et al.* 1978, 1982; Bumann *et al.* 1984, 1986; Europe-Finner & Newell 1985). Malchow *et al.* (1982) present evidence that calcium is necessary for cyclic-AMP-induced migration, and that it is the increase of cytosol calcium which causes the change of cell shape that underlies the observed light scattering. These authors also report that the addition of ionophore to suspensions of oscillating cells causes phase changes in the light scattering response. Bumann *et al.* (1984) have shown that the extracellular calcium concentration also oscillates in suspensions that exhibit oscillations in light scattering. They report that the period of these oscillations ranges from 6 to 11 min, that the addition of cyclic AMP induces a transient uptake of calcium by pre-aggregation cells, and that intracellular calcium levels can increase approximately thirtyfold in 5 s. Furthermore, if the

PHILOSOPHICAL TRANSACTIONS OF THE ROYAL SOCIETY B BIOLOGICAL SCIENCES

external cyclic AMP stimulus is maintained the cells remain loaded with calcium. The latter observation is predicted by the model we developed in (I) and (II). More recently, Europe-Finner & Newell (1985) have investigated the kinetics of the calcium uptake described by Malchow *et al.* In these experiments *Dictyostelium* cells suspended in calcium-free buffer are exposed to either a sudden increase in the external calcium concentration, or a sudden increase in both external calcium and cyclic AMP concentrations. The rate of calcium uptake is then monitored for about 1 min immediately after the addition of calcium. The authors interpret their results as showing that calcium uptake involves facilitated diffusion, and they compute the kinetic constants for this process. Their observation of facilitated diffusion has led us to modify the model used in (I) and (II) to incorporate this type of transport, as is discussed later in §§2 and 3. The authors also conclude that stimulation by cyclic AMP does not stimulate the initial rate of calcium uptake by cells, but does increase the duration of uptake, with the result that the total uptake of calcium is increased. The validity of this conclusion depends heavily on knowing the initial time course (the first few seconds) of calcium uptake accurately, which may be affected by changes in the cyclic AMP concentration on the same time scale. Although the cyclic AMP concentrations used in the experiments are large, phosphodiesterase on the cell membrane will degrade the external cyclic AMP rapidly (Pate *et al.* 1989), thereby causing cyclic AMP concentrations to rise more slowly close to the cell membrane than in the bulk fluid.

Europe-Finner & Newell also find that there is no change in calcium uptake between vegetative and aggregation competent cells. From details of the early time-course of the calcium influx they conclude that the initial uptake of calcium cannot be the trigger for early chemotactic events. Instead they suggest that desequestration of calcium from intracellular stores may be important for early chemotactic events such as the cyclic GMP response. They do not discuss the relation between calcium influx and relay adaptation, but the time course of the influx they observe is compatible with the role of calcium in controlling relay adaptation postulated in our model. This point is discussed further in the context of the generalizations described in §5.

Bumann *et al.* (1986) have investigated the phase relations between the calcium oscillations and other oscillating components such as cyclic AMP in suspensions. They find that the maximum of the total cyclic AMP concentration precedes the minimum in the extracellular calcium concentration by about 30 s, which is also consistent with our model (cf. §4). Bumann *et al.* also discovered two types of external calcium oscillation, a large amplitude spike-shaped oscillation associated with cyclic AMP oscillations, and a smaller amplitude sinusoidal external calcium oscillation not accompanied by a measurable cyclic AMP oscillation. We discuss these observations in §§4 and 6.

An outline of the remainder of the paper is as follows. In §2 we present the governing equations for the model and discuss some general properties of the solutions. In §3 we discuss the constraints placed on parameters by the requirement of perfect adaptation, and give a detailed analysis of the time course of adaptation. A qualitative analysis of the model, which shows how periodic oscillations can develop, is done in §4. There we also present numerical results that show the model reproduces the essential features of the experimental results very well. After that, we study the parametric dependence of the period and amplitude of the periodic solutions on several parameters that can either be controlled experimentally or which are known to vary with the developmental age of the cell.

In §5, we discuss certain extensions of the basic model. Firstly, the results given in §4 pertain

to suspensions that are uniform, but there is evidence that aggregation of cells into small clusters may precede the onset of cyclic AMP and light scattering oscillations (Gerisch 1968; Weijer *et al.* 1984; Bumann *et al.* 1986; P. Devreotes, personal communication). Thus we describe a modification of the extracellular equations that incorporates the formation of small aggregates of cells. Secondly, as we noted previously, only a small proportion of cells oscillate autonomously in fields of aggregating cells (Raman *et al.* 1976). To allow for this possibility in suspensions we introduce two populations of cells, one that is relay competent (but not oscillatory) and one that is capable of autonomous oscillations. As we shall see, periodic oscillations can exist even when there is only a small fraction of pacemaker cells. Lastly, we consider the effect of time delays in some of the control processes. In our basic model the effect of calcium on adenylate cyclase is rapid, but in reality it is possible that calcium acts more slowly, for instance via calmodulin. The inclusion of a time delay in the action of calcium on adenylate cyclase is one way to model this effect. We also consider a delay between binding of cyclic AMP to membrane receptors and the subsequent activation of adenylate cyclase and calcium channels to model slower transduction steps. A discussion of the biological significance of our results and a comparison with other work are given in §6.

2. The mathematical model

In this section we extend the model for the calcium–cyclic-AMP control network in *D. discoideum* developed in (I) and (II) so as to be applicable to the suspension experiments. The network of the major processes and the control pathways in the expanded model is shown in figure 1.

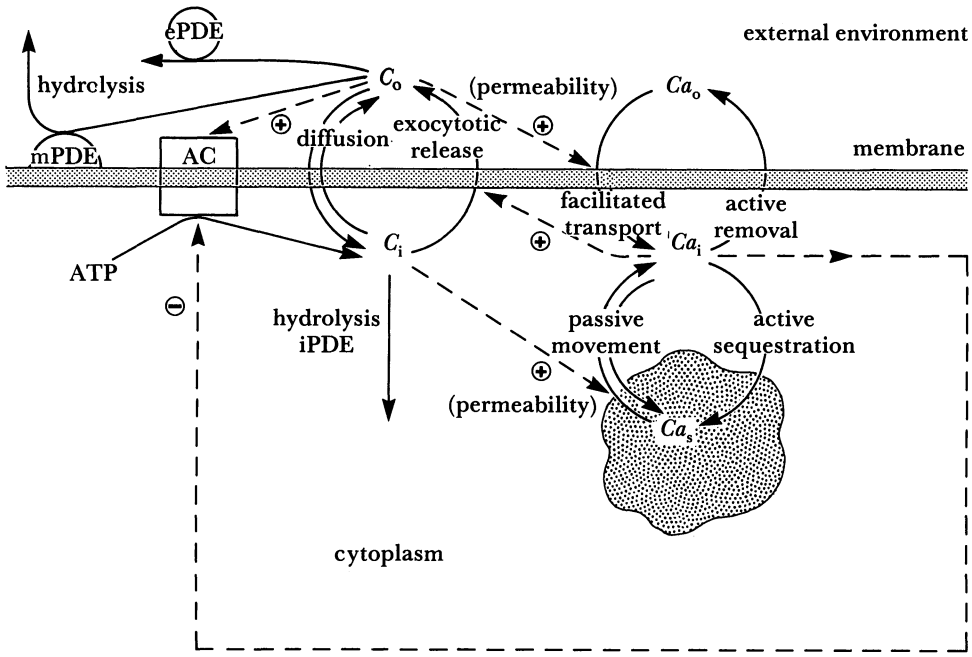

FIGURE 1. A schematic of the calcium-cyclic AMP control network in *Dictyostelium discoideum* proposed in (I) and (II) and modified herein. Solid arrows indicate the chemical reaction and transport pathways, broken lines indicate the control pathways. AC, adenylate cyclase; ATP, adenosine triphosphate; C_o, concentration of extracellular cyclic AMP; C_i, concentration of cytosol cyclic AMP; Ca_o, concentration of extracellular calcium; Ca_i, concentration of cytosol calcium; Ca_s, concentration of sequestered intracellular calcium; ePDE, extracellular free phosphodiesterase; iPDE, cytoplasmic phosphodiesterase; mPDE, membrane bound extracellular phosphodiesterase.

2.1. *The equations for the intracellular dynamics*

Because the equations for the intracellular variables are independent of whether or not the concentration of extracellular cyclic AMP is clamped, we give a brief description of the processes that appear in the equations for these variables first. The major reaction and transport steps are as follows (see table 1 for the definitions of each symbol).

$$\left.\begin{aligned}
&C_i + [iPDE] \underset{k_{-5}}{\overset{k_5}{\rightleftharpoons}} [C_i iPDE] \overset{k_5'}{\rightarrow} [iPDE];\\
&S \overset{\bar{V}}{\rightarrow} C_i \quad \text{production of cyclic AMP by adenylate cyclase;}\\
&C_v \overset{\bar{f}_v}{\rightarrow} C_o \quad \text{exocytosis;}\\
&C_i \overset{\bar{f}_2}{\leftrightarrow} C_v \quad \text{vesicle loading;}\\
&C_i \overset{h}{\leftrightarrow} C_o \quad \text{transmembrane diffusion;}\\
&Ca_i \underset{\bar{g}_2}{\overset{\bar{g}_1}{\rightleftharpoons}} Ca_o \quad \text{calcium exchange between cytoplasm and exterior;}\\
&Ca_s \underset{\bar{g}_4}{\overset{\bar{g}_3}{\rightleftharpoons}} Ca_i \quad \text{calcium exchange between cytoplasm and sequestration.}
\end{aligned}\right\} \tag{1}$$

The functions $\bar{g}_3$ and $\bar{g}_4$, which describe sequestration and desequestration of calcium, and the function describing the calcium pump, which is included in $\bar{g}_2$, are the same as used in (II). There it was also assumed that calcium enters the cell via passive diffusion through the cell membrane, but in light of Newell's results (Europe-Finner & Newell 1985) we replace this by facilitated transport. We assume that the velocity of this transport step is an increasing function of the external cyclic AMP concentration; and thus take

$$\bar{g}_2(Ca_o, C_o) - \bar{g}_1(Ca_i, C_o) = \bar{R}_1(C_o)\frac{Ca_o}{K_{FCa} + Ca_o} - V_{pump}\frac{Ca_i^{q_4}}{K_{pump}^{q_4} + Ca_i^{q_4}}, \tag{2}$$

where $\bar{R}_1(C_o)$ is an increasing function. In (II) we used a simple rational expression for this function, but here we use the form

$$\bar{R}_1(C_o) = V_{m1}\left(\frac{R_I + k_I C_o}{1 + k_I C_o}\right)\left(\frac{R_{I1} + k_{I1} C_o}{1 + k_{I1} C_o}\right). \tag{3}$$

This reduces to the form used in (II) when $R_{I1} = 1$. The function $\bar{f}_2(x_2)$, which represents the rate of loading of vesicles by cyclic AMP, will also be changed. In (II) we used the standard Hill form, but in §3 we discuss a simpler choice for $\bar{f}_2$. For the remainder of this section we shall only assume that $\bar{f}_2$ is an increasing function and that $\bar{f}_2(0) = 0$.

The details of the molecular model for the adenylate cyclase are discussed in the following section. Here it suffices to note that the system of ordinary differential equations that governs the time dependence of all species shown in figure 1 and the intermediate species for the various enzyme steps is too large for direct analysis. However, the number of equations can be greatly reduced by singular perturbation techniques, and thus we assume that the pseudo-steady-state

hypothesis applies as usual to the intermediates in all enzymic reactions. As a result we can represent the velocity of adenylate cyclase as $\bar{V}(C_o, Ca_i)$. This function will have the properties that (i) $\bar{V} > 0$ for all non-negative values of its arguments, and (ii) $\bar{V}_{max} \equiv \sup_{u,v \geqslant 0} \bar{V}(u,v)$ is bounded.

The applicability of this reduction has been justified rigorously for the model in (II), and a similar procedure applied here leaves us with a reduced system which has only three dependent variables. These are the concentration of intracellular cyclic AMP, the concentration of cytosol calcium and the concentration of sequestered calcium. We denote the dimensionless forms of these variables by x_2, x_3, and x_4 respectively (see table 2). In making this reduction we have assumed that the vesicle compartment equilibrates rapidly with the cytosol compartment. In (II) we considered the effects of a slower response in the vesicle compartment, which include a lag between the rise in intracellular cyclic AMP and the rise in secretion rate, and a reduced degradation of intracellular cyclic AMP by intracellular phosphodiesterase. In that paper x_5 denotes the dimensionless concentration of cyclic AMP in the vesicles, which is here related to x_2 through the pseudo-steady-state hypothesis. For the reader's convenience the complete set of dimensionless quantities is given in table 1, and the non-dimensional variables and parameters are defined in table 2.

2.2. *The equations for the extracellular dynamics*

In the perfusion experiments of Devreotes *et al.* (1979) the external cyclic AMP concentration is a prescribed function of time and the external calcium concentration is held fixed. If we denote by x_1 and x_6 the dimensionless concentrations of extracellular cyclic AMP and calcium (see table 2), the equations applicable to the perfusion experiments are

$$x_1 \equiv x_1(t) \quad \text{and} \quad x_6 \equiv \text{constant}, \tag{4}$$

together with the following system of equations for the intracellular variables.

$$\left.\begin{aligned}
\frac{dx_2}{d\tau} &= V(x_1, x_3) + H(x_1 - R_H x_2) - f_2(x_2) - V_{PI}\left(\frac{x_2}{1+x_2}\right), \\
\frac{dx_3}{d\tau} &= R_1(x_1)\left(\frac{x_6}{K_F + x_6}\right) - V_{PU}\left(\frac{x_3^{q_4}}{K_{PU}^{q_4} + x_3^{q_4}}\right), \\
&\quad + V_S\left(\frac{R_S + K_S x_2}{1 + K_S x_2}\right)(x_4 - x_3) - V_{SA}\left(\frac{x_3^{q_5}}{1 + x_3^{q_5}}\right), \\
\frac{dx_4}{d\tau} &= \left(\frac{R_c}{1 - R_c}\right)\left(V_{SA}\left(\frac{x_3^{q_5}}{1 + x_3^{q_5}}\right) - V_S\left(\frac{R_S + K_S x_2}{1 + K_S x_2}\right)(x_4 - x_3)\right).
\end{aligned}\right\} \tag{5}$$

The functions V and f_2 above are the dimensionless forms of $\bar{V}$ and $\bar{f}_2$ mentioned previously and

$$R_1(x_1) = V_I\left(\frac{R_I + K_I x_1}{1 + K_I x_1}\right)\left(\frac{R_{I1} + K_{I1} x_1}{1 + K_{I1} x_1}\right). \tag{6}$$

To model the suspension experiments we assume for the present that the suspension is well mixed, and we derive the applicable equations for the dimensionless external concentrations x_1 and x_6. The effects of partial aggregation of cells are considered in §5. In most suspension experiments there is no addition or removal of calcium or cyclic AMP, aside from pulses of one

Table 1. Definitions of dimensional variables and parameters

(The dimension of each variable is given in square brackets: M, mass, L, length and T, time.)

α	Hill coefficient for membrane bound phosphodiesterase (a dimensionless positive number)
A_{cl}	effective surface area of a cluster through which calcium and cyclic AMP diffuse [L^2]
A_c	surface area of a cell [L^2]
A_s	total surface area of the sequestration compartment [L^2]
$Ca_i(t)$	cytoplasmic calcium ion concentration [M/L^3]
$Ca_o(t)$	calcium ion concentration in the external compartment (or in the external clump compartment) [M/L^3]
$Ca_0'(t)$	calcium ion concentration in cell-free extracellular compartment (applies to clumping only) [M/L^3]
$Ca_s(t)$	sequestered calcium ion concentration [M/L^3]
Ca_{tot}	total calcium ion present in the experiment [M]
$C_i(t)$	cytoplasmic cAMP concentration [M/L^3]
$[C_i iPDE](t)$	concentration of intracellular cAMP – phosphodiesterase complex [M/L^3]
$C_o(t)$	concentration of cAMP in external compartment (or in external clump compartment) [M/L^3]
$C_o'(t)$	cyclic AMP concentration in the cell-free extracellular compartment (applies to clumping only) [M/L^3]
$[C_o ePDE](t)$	external cAMP – free phosphodiesterase complex concentration [M/L^3]
$[C_o mPDE](t)$	external cAMP – membrane phosphodiesterase complex concentration per unit surface area [M/L^2]
$C_v(t)$	concentration of cAMP in vesicle compartment [M/L^3]
$[ePDE](t)$	concentration of free external phosphodiesterase [M/L^3]
$ePDE_o$	total free external phosphodiesterase per cell [M]
$\bar{f}_1(C_v, Ca_i)$	rate per unit area of transport of cAMP from vesicle to the external compartment [$(M/L^2)T^{-1}$]
$\bar{f}_2(C_i, Ca_i)$	rate per unit area of transport of cAMP from cytoplasmic to vesicle compartment [$(M/L^2)T^{-1}$]
$\bar{g}_1(Ca_i, C_o)$	rate per unit area of transport of cytoplasmic calcium to exterior compartment [$(M/L^2)T^{-1}$]
$\bar{g}_2(Ca_o, C_o)$	rate per unit area of transport of exterior calcium to cytoplasm [$(M/L^2)T^{-1}$]
$\bar{g}_3(Ca_i, C_i)$	rate per unit area of transport of cytoplasmic calcium into sequestration compartment [$(M/L^2)T^{-1}$]
$\bar{g}_4(Ca_s, C_i)$	rate per unit surface area of transport of sequestered calcium to cytoplasm [$(M/L^2)T^{-1}$]
h	permeability of cell membrane to cAMP [L/T]
$[iPDE](t)$	concentration of cytoplasmic phosphodiesterase [M/L^3]
$iPDE_o$	total intracellular phosphodiesterase [M]
k_{Ca}	diffusion constant for calcium between cell-free fluid and clump [L/T]
k_{cAMP}	diffusion constant for cyclic AMP between cell-free fluid and clump [L/T]
k_I, k_{II}	parameters relating changes in external cyclic AMP to changes in the cell membrane permeability to calcium [L^3/M]
k_S	parameter relating changes in intracellular cyclic AMP to changes in the permeability of the sequestration compartment wall to calcium [L^3/M]
K_e	effective Michaelis constant for free external phosphodiesterase $K_i = (k_6' + k_{-6})/k_6$) [$M/L^3$]
K_{FCa}	Michaelis constant for the facilitated diffusion process [M/L^3]
k_i, k_{-i}, k_i'	phosphodiesterase kinetic constants, $i = 0$ denotes external membrane-bound enzyme, $i = 5$ denotes internal enzyme, and $i = 6$ denotes free extracellular enzyme
K_i	effective Michaelis constant for intracellular phosphodiesterase $K_i = (k_5' + k_{-5})/k_5$ [M/L^3]
K_m	effective Michaelis constant of membrane-bound phosphodiesterase $K_m = [(k_0' + k_{-0})/k_0]^{1/\alpha}$ [M/L^3]
K_{pump}	effective Michaelis constant of active calcium pump (exocytosis) [M/L^3]
K_{seq}	effective Michaelis constant of calcium sequestration [M/L^3]
$[mPDE](t)$	concentration per unit surface area of membrane-bound (external) phosphodiesterase [M/L^2]
$mPDE_o$	total concentration of membrane-bound phosphodiesterase [M/L^2]
N	number of cells in suspension [a dimensionless positive integer]
n	number of cells in a clump [a dimensionless positive integer]
$q_1, \ldots, q_5$	Hill coefficients [dimensionless integers]
R_I, R_{II}	parameters giving ratio of minimum to maximum permeability of the cell wall to calcium [dimensionless, less than 1]
R_S	ratio of minimum to maximum permeability of the sequestration compartment wall to calcium [dimensionless, less than 1]
t	time [T]
V_c	total volume of cytoplasmic compartment [L^3]
V_o	total volume of external compartment [L^3]
V_{m1}	maximum permeability of the cell wall to calcium [L/T]
V_{m2}	maximum permeability of the sequestration compartment wall to calcium [L/T]
V_{pump}	maximum velocity of the active exocytotic calcium pump [M/L^2T]
V_s	total volume of sequestration compartment [L^3]
V_{seq}	maximum velocity of the active sequestration calcium pump [M/L^2T]

PHILOSOPHICAL TRANSACTIONS OF THE ROYAL SOCIETY B BIOLOGICAL SCIENCES

TABLE 2. DIMENSIONLESS QUANTITIES

2.1. dimensionless variables

$$x_1 = C_o/K_m \qquad x_6 = Ca_o/K_{seq}$$
$$x_2 = C_i/K_i \qquad x_7 = C'_o/K_m$$
$$x_3 = Ca_i/K_{seq} \qquad x_8 = Ca'_o/K_{seq}$$
$$x_4 = Ca_s/K_{seq} \qquad \tau = k_5\,\mathrm{i}PDE_o\,t = t/T$$

2.2. dimensionless constants

$$H = \{hA_c K_m\}/\{k_5(\mathrm{i}PDE_o)\,V_c K_i\} \qquad R_H = K_i/K_m$$
$$K_{Ca} = \{A_{cl} k_{Ca}\}/\{nV_c k_5(\mathrm{i}PDE_o)\} \qquad V_{PE} = k'_6(\mathrm{e}PDE_o)/\{k_5(\mathrm{i}PDE_o)\,K_m V_c\}$$
$$K_{CP} = \{A_{cl} k_{cAMP}\}/\{nV_c k_5(\mathrm{i}PDE_o)\} \qquad V_I = \{A_c V_{m1}\}/\{k_5(\mathrm{i}PDE_o)\,V_c\}$$
$$K_I = k_I K_m \qquad V_{PI} = k'_5/(k_5 K_i)$$
$$K_{II} = k_{II} K_m \qquad V_{PO} = \{k'_o(\mathrm{m}PDE_o)\,A_c\}/\{k_5(\mathrm{i}PDE_o)\,V_c K_m\}$$
$$K_F = K_{FCa}/K_{seq} \qquad V_{PU} = \{A_c V_{pump}\}/\{k_5(\mathrm{i}PDE_o)\,V_c K_{seq}\}$$
$$K_{PU} = K_{pump}/K_{seq} \qquad V_{SA} = \{A_s V_{seq}\}/\{k_5(\mathrm{i}PDE_o)\,V_c K_{seq}\}$$
$$K_S = k_S K_i \qquad V_S = \{A_s V_{m2}\}/\{k_5(\mathrm{i}PDE_o)\,V_c\}$$
$$R_c = V_c/(V_c + V_s) \qquad \bar{x}_6 = Ca_{tot}/(K_{seq}\{N(V_c + V_s) + V_o\})$$
$$R_e = K_e/K_m \qquad \rho = N(V_c + V_s)/\{N(V_c + V_s) + V_o\}$$

ϵ ratio of extracellular volume to cell volume in a clump (see §5)
K_{VP} dimensionless apparent Michaelis constant for vesicle loading
μ ratio of numbers of cell types in two population studies (see §5)
τ_i, $i = 1, 2$ dimensionless delay times (see §5)
V_{sw} dimensionless velocity for vesicle loading at switch point
V_1 scale factor for dimensionless adenylate cyclase velocity
V_1^i, $i = 1, 2$ scale factor for dimensionless adenylate cyclase velocity in two population studies (see §5)
V_{VP} dimensionless scale factor for the velocity of vesicle loading
x_{sw} dimensionless intracellular cyclic AMP concentration at switch point
$\tilde{x}_6$ reference non-dimensional calcium concentration for perfect adaptation (see §2)

or both species introduced initially. Thus calcium is conserved, which leads to the following condition:

$$NV_c\,Ca_i + NV_s\,Ca_s + V_o\,Ca_o = Ca_{tot}. \tag{7}$$

Here N is the number of cells in a suspension, V_c, V_s, and V_o are the volumes of the cytoplasm, of the calcium sequestration compartment within a cell, and of the external fluid, respectively, and Ca_{tot} represents the total amount of calcium present. Because the system is also closed for cyclic AMP, all extracellular cyclic AMP is released from the cells, either via the vesicles or by passive diffusion. This extracellular cyclic AMP is hydrolysed by either a membrane-bound form of phosphodiesterase or by a free form in the extracellular fluid. The latter enzyme is known to be Michaelian (Pannbacker & Bravard 1972), but the surface bound form exhibits negative cooperativity (Malchow *et al.* 1975). The reaction steps for these enzymes are as follows:

$$\alpha C_0 + [\mathrm{m}PDE] \underset{k_{-0}}{\overset{k_0}{\rightleftharpoons}} [C_0\,\mathrm{m}PDE] \overset{k'_0}{\rightarrow} [\mathrm{m}PDE] \tag{8}$$

and

$$C_0 + [\mathrm{e}PDE] \underset{k_{-6}}{\overset{k_6}{\rightleftharpoons}} [C_0\,\mathrm{e}PDE] \overset{k'_6}{\rightarrow} [\mathrm{e}PDE]. \tag{9}$$

Here $[\mathrm{e}PDE]$ represents the concentration of phosphodiesterase in the external fluid, and $[C_0\,\mathrm{e}PDE]$ represents the concentration of the cyclic AMP phosphodiesterase complex. Similar definitions hold for $[\mathrm{m}PDE]$ and $[C_0\,\mathrm{m}PDE]$ (see table 1). We assume that the total amount of free phosphodiesterase present is proportional to the number of cells in suspension. Thus for a fixed cell density the free form is present at a constant concentration throughout the duration of the experiment, and we use the Michaelis constant for the inhibited form (Chassy 1972; Kessin *et al.* 1979).

PHILOSOPHICAL TRANSACTIONS OF THE ROYAL SOCIETY B BIOLOGICAL SCIENCES

With the above assumptions and an application of the pseudo-steady-state hypothesis to the intermediate complexes in (8) and (9), we can derive an equation governing the concentration of extracellular cyclic AMP. Consequently, the dimensionless equations governing the dynamics of suspensions are as follows:

$$\left.\begin{aligned}
\frac{dx_1}{d\tau} &= R_c\left(\frac{\rho}{1-\rho}\right)\left(R_H f_2(x_2) - V_{PO}\left(\frac{x_1^\alpha}{1+x_1^\alpha}\right) + HR_H(R_H x_2 - x_1)\right.\\
&\qquad \left. - V_{PE}\left(\frac{x_1}{R_e + x_1}\right)\right)\\
\frac{dx_2}{d\tau} &= V(x_1, x_3) + H(x_1 - R_H x_2) - f_2(x_2) - V_{PI}\left(\frac{x_2}{1+x_2}\right)\\
\frac{dx_3}{d\tau} &= R_1(x_1)\left(\frac{x_6}{K_F + x_6}\right) - V_{PU}\left(\frac{x_3^{q_4}}{K_{PU}^{q_4} + x_3^{q_4}}\right)\\
&\qquad + V_S\left(\frac{R_S + K_S x_2}{1 + K_S x_2}\right)(x_4 - x_3) - V_{SA}\left(\frac{x_3^{q_5}}{1+x_3^{q_5}}\right)\\
\frac{dx_4}{d\tau} &= \left(\frac{R_c}{1-R_c}\right)\left(V_{SA}\left(\frac{x_3^{q_5}}{1+x_3^{q_5}}\right) - V_S\left(\frac{R_S + K_S x_2}{1 + K_S x_2}\right)(x_4 - x_3)\right)\\
x_6 &= \left(\frac{1}{1-\rho}\right)(\bar{x}_6 - R_c \rho x_3 - (1-R_c)\rho x_4).
\end{aligned}\right\} \tag{10}$$

The definition of each of the dimensionless parameters in the above equations is given in table 2.

The first step in the analysis of (10) is to show that solutions subject to non-negative initial data remain non-negative and bounded for all positive time. The verification that the flow of (10) preserves non-negativity is straightforward and is left to the reader. To show the existence of a compact attracting set we proceed as follows. Because the calcium concentrations remain positive and obey the conservation condition given by (7), we can conclude that they remain bounded for all time provided that ρ is such that $0 < \rho < 1$, which is certainly the case because ρ is the normalized density. By considering the sum of the equations for x_1 and x_2 one can show that the quantity $x_1 + \rho/(1-\rho)\, R_c R_H x_2$ remains bounded for all time provided that the phosphodiesterase velocities V_{PO}, V_{PE} and V_{PI} are sufficiently large compared with the maximal velocity of adenylate cyclase. We always assume that the rates of degradation of cyclic AMP are large enough to guarantee this. In view of the fact that x_1 and x_2 are positive, the preceding shows that $x_1, \ldots, x_4$ and x_6 can be bounded uniformly in time, with bounds that depend only on the initial data.

3. The mechanism of adaptation

In (II) we analysed the equations for simulating perfusion experiments with certain choices of V, R_1, and f_2, and showed that the model can explain many of the experimental results of Devreotes *et al.* (1979). In this section we discuss an extension of this model that incorporates more general functional forms for the adenylate cyclase velocity and calcium influx, and again show that it can account for the results from perfusion experiments. In addition, we investigate how the component processes shape the response to a stimulus.

3.1. *Constraints imposed by adaptation*

In this paper we adopt the following dimensionless form for the rate of production of adenylate cyclase:

$$V(x_1, x_3) = V_1 \frac{ax_1^2 + bx_1 + c}{x_3(dx_1^2 + ex_1 + f) + (gx_1^2 + hx_1 + 1)}. \tag{11}$$

This is done to decrease the range of calcium variation needed to guarantee adaptation to external cyclic AMP stimuli ranging from 10^{-9} to 10^{-6} M (cf. (II)). This function can be obtained as a special case of the general model derived in ((II), p. 133), but it can also be obtained from the simple molecular model shown in figure 2. After applying the pseudo-steady-state hypothesis to the differential equations derived from the kinetic steps shown in figure 2 one arrives at a simple rational function of C_o and Ca_i for the rate function, and (11) is simply the dimensionless form of this function.

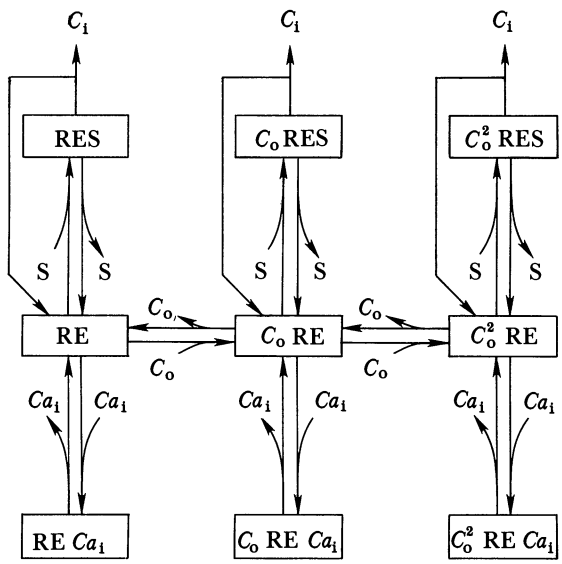

FIGURE 2. A diagram showing a simple molecular model of adenylate cyclase that gives rise to the rate function given at (11). (See also (II), p. 133.) Ca_i, cytoplasmic calcium; C_i, intracellular cyclic AMP; C_o, extracellular cyclic AMP; E, adenylate cyclase catalytic unit; R, cell surface cyclic AMP receptor; S, adenylate cyclase substrate assumed constant. Each symbol represents a complex of the molecular species composing the symbol. It is assumed that the receptor and enzyme are precoupled, or if they are uncoupled that coupling is rapid compared with other steps. Receptor–enzyme complexes bound with calcium are assumed to have no catalytic activity. Extracellular cyclic AMP increases the catalytic activity in the absence of calcium. This type of model was discussed in detail in (II).

The parameters $a \ldots h$ and V_1 in (11) are all independent, and we shall choose them so as to guarantee perfect adaptation in the perfusion experiments described in §1. As in (II), we require that the secretion rate exhibit perfect adaptation to any constant level of extracellular cyclic AMP at a particular fixed external calcium concentration (say $x_6 = \tilde{x}_6$). Because the cyclic AMP release function is independent of calcium, it follows that perfect adaptation occurs only if the steady state level of intracellular cyclic AMP (x_2) is independent of the fixed extracellular cyclic AMP concentration (x_1). This in turn implies that the velocity of adenylate cyclase must be independent of x_1, to first order in H, at a steady state.

An analysis of the steady states allows us to derive the relations between the coefficients in

the adenylate cyclase velocity and the coefficients in the calcium equation that will ensure perfect adaptation. The steady-state equation $dx_3/d\tau = 0$ can be solved to give x_3 as a function of x_1. Upon substituting this expression for x_3 in (11) and requiring that the resulting rational function of x_1 be independent of x_1, one is lead to certain relations between the coefficients of the numerator and denominator of the rate function. From this analysis one finds that there are only four free parameters in the rate function: the basal rate of production V_1, and three of the eight positive non-dimensional quantities $a \ldots h$, which we choose to be f, g and h. To simplify the resulting expressions for the dependent parameters let

$$\left.\begin{aligned} \Omega &= V_{\mathrm{I}} K_{\mathrm{PU}} \tilde{x}_6/(V_{\mathrm{PU}}(K_{\mathrm{F}}+\tilde{x}_6)),\\ \chi &= -\tilde{x}_6 V_{\mathrm{I}}/(V_{\mathrm{PU}}(K_{\mathrm{F}}+\tilde{x}_6)),\\ \alpha &= \Omega R_{\mathrm{I}} R_{\mathrm{I1}},\\ \beta &= \Omega(R_{\mathrm{I}} K_{\mathrm{I1}} + R_{\mathrm{I1}} K_{\mathrm{I}}),\\ \gamma &= \Omega K_{\mathrm{I}} K_{\mathrm{I1}},\\ \delta &= 1+\chi R_{\mathrm{I}} R_{\mathrm{I1}},\\ \mu &= K_{\mathrm{I}} + K_{\mathrm{I1}} + \chi(R_{\mathrm{I}} K_{\mathrm{I1}} + R_{\mathrm{I1}} K_{\mathrm{I}})\\ \text{and}\quad \rho &= (1+\chi)\, K_{\mathrm{I}} K_{\mathrm{I1}}. \end{aligned}\right\} \tag{12}$$

Further, let

$$\left.\begin{aligned} r_1 &= \beta\delta - \alpha\mu,\\ r_2 &= \gamma\delta - \rho\alpha,\\ r_3 &= \gamma\mu - \beta\rho,\\ r_4 &= r_2^2 - r_1 r_3\\ \text{and}\quad r_5 &= r_2 r_3 - \mu r_1 r_3/\delta + \rho r_1 r_2/\delta. \end{aligned}\right\} \tag{13}$$

Then one finds that $a \ldots e$ are given in terms of f, g and h as follows:

$$\left.\begin{aligned} a &= \gamma f(\delta r_2 r_5/r_4 - \rho r_1/(r_3\delta^2)) + g,\\ b &= \alpha e/\delta + r_1 f/\delta^2 + h,\\ c &= 1+\alpha f/\delta,\\ d &= f(\rho\delta r_2 r_5/r_4 - \rho^2 r_1/(r_3\delta^2))\\ \text{and}\quad e &= r_5 f/r_4. \end{aligned}\right\} \tag{14}$$

Here $\tilde{x}_6$ is the non-dimensional external calcium concentration at which perfect adaptation occurs. Adaptation will be close to perfect for external calcium concentrations close to this chosen reference concentration. The interested reader can consult (II) for more discussion of this type of enzyme model, and a more detailed discussion of perfect adaptation.

The remaining function to be specified is f_2, which gives the rate of secretion of cyclic AMP. For this we use the following dimensionless function.

$$f_2(x_2) = \begin{cases} V_{VP}\dfrac{(x_2 - x_{sw})}{K_{VP} + (x_2 - x_{sw})} + V_{sw} & \text{if} \quad x_2 \geqslant x_{sw}, \\ \left(\dfrac{V_{sw}}{x_{sw}}\right) x_2 & \text{if} \quad x_2 < x_{sw}. \end{cases} \tag{15}$$

This choice is based on the supposition that the number of vesicles present is small at low cyclic AMP and the rate of transport is low, whereas above a certain level vesicles are produced or activated by the cell and transport is proportionately more rapid. The foregoing function has a discontinuity in slope at the point $x_2 = x_{sw}$, and in the numerical computations described later we use a smoothed version of this function.

3.2. *Linear analysis of adaptation*

We are now in a position to discuss the factors that control the dynamics of the secretion response. Firstly, let us consider the case in which the sequestration compartment equilibrates rapidly, in which case it can be removed by singular perturbation. Suppose that the system is at steady state, and let x_1 be increased to a level at which the corresponding steady-state value of x_3 is much smaller than K_{PU} (in fact, this assumption is satisfied quite well for our parameter values, as long as $x_1 \leqslant 1$). In this case the calcium pump is far from saturation, and an upper bound to x_3 is given by the solution of the equation

$$\frac{dx_3}{d\tau} = \underbrace{V_I\left(\frac{R_I + K_I x_1}{1 + K_I x_1}\right)\left(\frac{R_{I1} + K_{I1} x_1}{1 + K_{I1} x_1}\right)\frac{x_6}{K_F + x_6}}_{\alpha(x_1)} - \underbrace{\frac{V_{PU}}{K_{PU}}}_{\beta} x_3.$$

Thus

$$x_3(\tau) = x_3(0)\, e^{-\beta\tau} + \{\alpha(x_1)/\beta\}\,(1 - e^{-\beta\tau}). \tag{16}$$

This equation implies that the half time for calcium loading of the cell is independent of stimulus strength, provided that V_{PU} and K_{PU} are independent of x_1. If external cyclic AMP were to inhibit the pump (via a decrease in V_{PU} or an increase in K_{PU}) the time to half maximum concentration of intracellular calcium would increase because β would decrease.

Similarly, if we linearize the secretion rate and use the binomial theorem to approximate the adenylate cyclase velocity, we find that the dynamic behaviour of x_2 is given approximately by the solution of the equation

$$dx_2/d\tau = V_0(1 + \gamma(x_1)\, e^{-\beta\tau}) - kx_2,$$

where V_0 is the activity before stimulation and $\gamma(x_1)$ reflects the activation of the enzyme. This equation results from some major simplifications of the full nonlinear equation for x_2, but at least for small changes in x_1 it captures the essential aspects of the x_2 dynamics. The solution of this equation can be written

$$x_2(\tau) - V_0/k = V_0\,\gamma(x_1)/(k - \beta)\,(e^{-\beta\tau} - e^{-k\tau}), \tag{17}$$

PHILOSOPHICAL TRANSACTIONS OF THE ROYAL SOCIETY B BIOLOGICAL SCIENCES

where we have used the fact that the system was at steady state before stimulation, which implies that $x_2(0) = V_0/k$. From (16) and (17) we see that the elapsed time to reach the maximum intracellular cyclic AMP concentration is given by

$$\tau_{\max} = 1/(k-\beta)\ln(k/\beta),$$

and that the maximum concentration is given by

$$x_2 = V_0/k + (V_0\gamma/\beta)(k/\beta)^{k/(\beta-k)}.$$

Under the standing assumption that the vesicle compartment equilibrates rapidly with the cytoplasmic compartment, $\tau_{\max}$ is also the elapsed time to maximum secretion rate.

It follows from the above relations that the time for half maximal response $\tau_{\frac{1}{2}}$ must satisfy the equation

$$\exp(-\beta\tau_{\frac{1}{2}}) - \exp(-k\tau_{\frac{1}{2}}) = ((k-\beta)/2\beta)(k/\beta)^{k/(\beta-k)}.$$

This equation has two solutions, the smaller of which is the time to half-maximal response on the upstroke and the larger of which is the time after stimulation at which the half maximal response occurs during the adaptation phase. These times are independent of the stimulus strength γ. A similar calculation shows that the time to reach *any* given fraction of the maximum response is independent of stimulus strength. The results given in the following subsection are based on parameter values for which k is much larger than β, and thus the time course of adaptation is essentially set by β. $\tau_{\max}$ cannot be set arbitrarily because β is determined by the adaptation response, and k must be chosen to give reasonable secretion rates in response to stimuli.

The above analysis shows how the characteristic times for the calcium and cyclic AMP systems enter into the various features of the response to a stimulus. Provided that the stimulus is not too large, the time to maximum response is independent of the stimulus strength, as was found experimentally by Dinauer *et al.* (1980*c*). Moreover, the size of the predicted response increases with γ, which implies that a larger stimulus will provoke a larger response as long as the enzyme and calcium pump are not saturated. This too is in agreement with the experimental results in Devreotes & Steck (1979).

This analysis also suggests that if the half-time for adaptation depends on the stimulus x_1, either the linear approximation must break down or k or β or both must depend on x_1. In particular, if external cyclic AMP inhibits the calcium pump, as has been conjectured (Europe-Finner & Newell 1985), then a longer half-life for decay at higher stimulus concentrations should result. A similar result would be seen if the pump is almost saturated by calcium at high external stimulus levels. Because this is not observed (Dinauer *et al.* 1980*c*), one would conclude from our model that external cyclic AMP does not inhibit the pump appreciably.

In the above analysis we have ignored the effects of saturation in any of the processes. The reader may consult (II) for a simple two-species caricature of the full system which includes saturation in some of the processes.

3.3. *Simulation of perfusion experiments*

The numerical results described shortly are obtained by using equations (4) and (5), under the assumption that the system is at steady state before the first stimulus. We use the parameter values given by table 3, which are close to those used in (II), but which have been modified to take into account the new functional forms.

PHILOSOPHICAL TRANSACTIONS OF THE ROYAL SOCIETY B BIOLOGICAL SCIENCES

Insight into adaptation in the full model can be obtained by using the response surface introduced in (II). Figure 3 shows a perspective view of a two-dimensional surface that is generated by plotting the adenylate cyclase velocity as a function of activator (external cyclic AMP) and inhibitor (cytosol calcium) concentrations. On this surface we have superimposed plots of two responses to different step increases in cyclic AMP. In both cases the system is started at steady state in the absence of external cyclic AMP and the external concentration is increased to 10^{-6} M either by a single step or by several smaller steps. A step increase in external cyclic AMP produces a rapid increase in the velocity of adenylate cyclase, which increases the cyclic AMP production and the rate of cyclic AMP secretion. The cytosolic

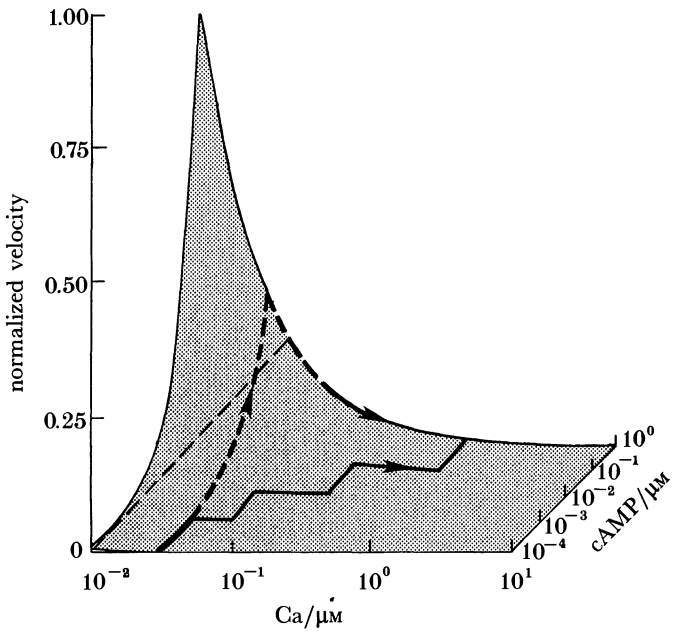

FIGURE 3. A response surface for the adenylate cyclase velocity given by (11). Shown here is a plot of the adenylate cyclase velocity as a function of extracellular cyclic AMP and cytosol calcium. The former is plotted logarithmically and ranges from 10^{-10} to 10^{-6} M. The broken curve is the response to a single step increase in extracellular cyclic AMP from 0 M to 10^{-6} M. The saw-tooth curve is the response to a number of smaller step increases from 0 to 10^{-6} M (see figure 4 for the exact sequence of steps). For each step in stimulus there is an immediate increase in the adenylate cyclase velocity, followed by a slow decrease as the cytoplasmic calcium concentration rises. Because the single and multiple step response traverse different parts of the response surface, these stimuli probe different parts of the enzyme dynamics.

TABLE 3. NUMERICAL VALUES OF SCALING AND DIMENSIONLESS CONSTANTS

3.1. scaling constants

K_i	10 μM	K_{seq}	3.0 μM
K_m	0.5 μM	T	0.5 min ($T = (k_5 i PDE_o)^{-1}$)

3.2. values of the dimensionless constants

α	1.0	K_{PU}	4.5	R_S	2.0×10^{-1}	V_{SA}	1.2×10^{4}
f	1.5×10^{3}	K_S	3.3×10^{3}	R_e	2.0×10^{3}	V_S	3.0×10^{2}
g	3.0×10^{1}	q_4	1	R_H	2.0×10^{1}	V_{sw}	3.0×10^{-3}
h	3.0×10^{2}	q_5	1	V_I	2.2×10^{2}	V_{VP}	5.0
H	1.5×10^{-6}	ρ	1.0×10^{-1}	V_{PI}	6.0×10^{-1}	V_1	1.2×10^{-1}
K_F	5.0×10^{2}	R_c	9.8×10^{-1}	V_{PE}	5.0×10^{3}	$\bar{x}_6$	1.0
K_I	2.0×10^{2}	R_I	1.5×10^{-1}	V_{PO}	1.0×10^{2}	$\tilde{x}_6$	1.0
K_{I1}	1.1	R_{I1}	3.3×10^{-2}	V_{PU}	1.25	x_{sw}	2.5×10^{-1}

PHILOSOPHICAL TRANSACTIONS OF THE ROYAL SOCIETY B BIOLOGICAL SCIENCES

calcium concentration rises on a slower timescale, inhibits adenylate cyclase, and thereby decreases the adenylate cyclase velocity to the basal level. Clearly the response to a single step and a multiple step experiment cover different parts of the surface, and hence these experiments probe different parts of the adenylate cyclase response. Thus any model must account for the responses to both single and multistep stimuli.

In figure 4 we show the computed response to a sequence of steps in external cyclic AMP concentration. Each step in the cyclic AMP stimulus elicits a temporary rise in cyclic AMP synthesis and release (see figure 4*a*, *c*), and this response is terminated by a slower rise in the cytoplasmic calcium concentration (see figure 4*d*). Devreotes & Steck (1979) find that the integrated response (i.e. total amount of cyclic AMP secreted) to step changes in external cyclic AMP depends only on the difference in the initial and final extracellular concentrations. We computed the integrated secretion rate for the multiple step input used in figure 4 and the integrated secretion rate for a single step change in external cyclic AMP from zero to 10^{-6} M (integrated over the same time), and found that the ratio of multistep to single step response is 0.84. This is well within the range measured by Devreotes *et al.*

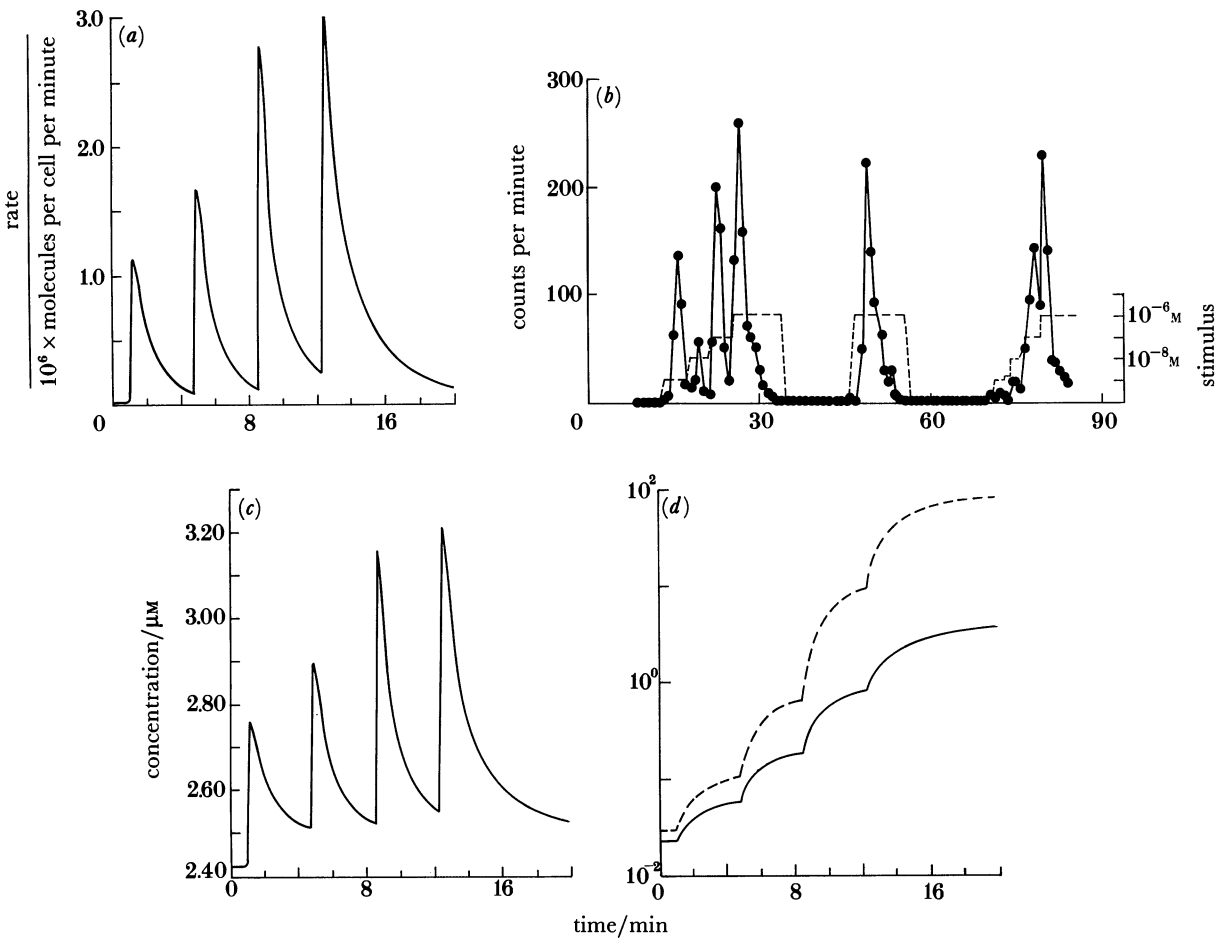

FIGURE 4. The response computed from (4) and (5) to a staircase input of extracellular cyclic AMP. Starting at $t = 1$ min, extracellular cyclic AMP was increased first from 0 to 10^{-9} M and then to 10^{-6} M in three tenfold steps of 225 s duration. Parameter values are as given in table 3. (*a*) Cyclic AMP secretion rate. This graph should be compared with the experimental results in (*b*). (*b*) Experimental measurements of the cyclic AMP secretion rate (redrawn from figure 8 of Devreotes & Steck (1979)). (*c*) Intracellular cyclic AMP. (*d*) Intracellular calcium (solid line: cytoplasmic calcium; broken line: sequestered calcium).

Figure 5 shows the results of modelling a perfusion experiment in which cells are stimulated by a step rise in external cyclic AMP from 0 to 10^{-9} M after 1 min, followed by a further increase to 10^{-6} M after 20 min. The ratio of the maximal responses to the two stimuli in the simulations is 16.8, versus a ratio of 14.6 for the experimental results given in figure 5*b*. The simulated responses appear to be too sharp and to peak too early when compared with the experimental results, but as we have pointed out in (II), the model describes the response of a single cell, whereas the experimental measurements record the response of a large population of cells. Slightly asynchronous cell behaviour and different parameters from cell to cell could result in a somewhat delayed and broadened peak for the response of the population compared with that of a single cell. In addition, the flow of fluid through the experimental apparatus will also tend to smooth the measured response of the experiment. We also note that the time course of adaptation for each peak in figure 5 is similar to that seen in figure 4, and much less dependent on the stimulus strength, in contrast with the results given in (II). This is in accordance with the observations of Dinauer *et al.* (1980*c*).

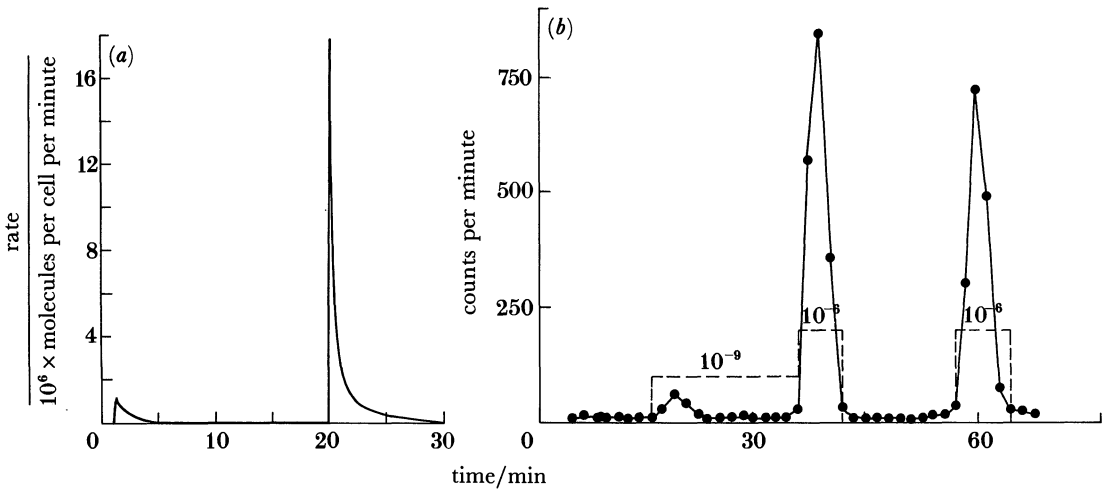

FIGURE 5. The response to stepwise stimuli of extracellular cyclic AMP computed by using (4) and (5). The system is started at steady state in the absence of extracellular cyclic AMP. After 1 min the extracellular cyclic AMP concentration is increased in a step to 10^{-9} M, and after 20 min increased in another step to 10^{-6} M. Parameter values are as given in table 3. (*a*) The computed secretion rate for a single cell. The computed response reaches the maximal value earlier and is sharper than the experimental response shown in (*b*). However, the smoothness of the observed response may be inherent in the averaging of the response over a large population of cells. (*b*) Experimentally observed secretion rate of cyclic AMP (redrawn from figure 7 of Devreotes & Steck (1979)).

Finally, in figure 6 we show the results of our simulations and the comparable results of an experiment of Dinauer *et al.* (1980*b*) that was designed to investigate de-adaptation. Again the present model produces better agreement with experimental results than the model given in (II).

The foregoing computations were all done using $V_1 = 0.12$. As we shall see in the next section, suspensions of cells with this value of V_1 are excitable but not capable of autonomous oscillations. However, it is not known whether or not the cells used by Devreotes *et al.* would oscillate if they were placed in a suspension. For this reason we have also done some numerical experiments on relay and adaptation using a V_1 large enough to make the cells oscillate autonomously if they were placed in suspension. The results show that all the qualitative features of the response are preserved, but of course the cyclic AMP concentrations and the secretion rate increase with increasing V_1.

PHILOSOPHICAL TRANSACTIONS OF THE ROYAL SOCIETY B BIOLOGICAL SCIENCES

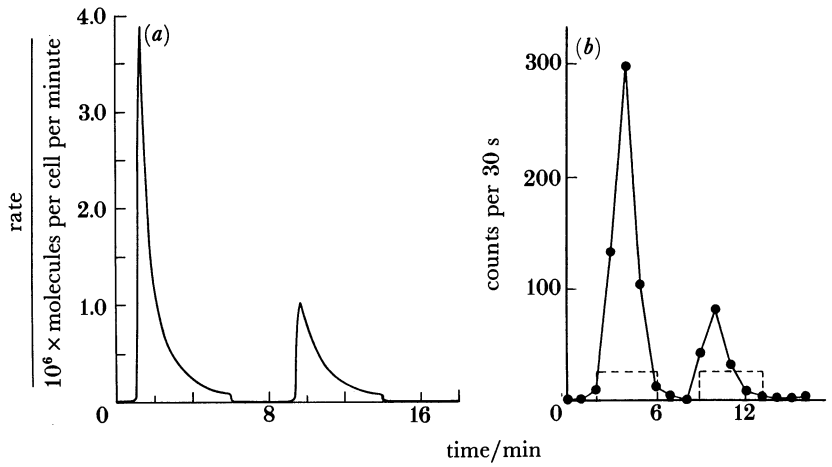

FIGURE 6. The response computed from (4) and (5) to two square-wave inputs of equal magnitude. The time-course of extracellular cyclic AMP is: 0 M ($t = 0$–1), 10^{-8} M ($t = 1$–6), 0 M ($t = 6$–9), and 10^{-8} M ($t = 8$–14). This experiment probes the time-course of deadaptation, because the magnitude of the response to the second stimulus depends upon the degree to which the cells have recovered from the first stimulus. Parameter values are as given in table 3. (*a*) The secretion rate per cell, which should be compared with the observed secretion rate shown in (*b*). (*b*) Experimentally observed secretion rate (redrawn from figure 2 of Dinauer *et al.* (1980*b*)).

4. Oscillations in homogeneous suspensions

The goal in this section is to gain a qualitative understanding of conditions under which the equations given at (10) may have periodic solutions. As may be anticipated, the existence of oscillatory solutions for certain parameter values is closely connected with the fact that the system is excitable for parameter values appropriate to the perfusion experiments, in the sense that small perturbations in the extracellular cyclic AMP concentration are amplified. However, the governing equations for suspensions are different than those used for the perfusion experiments and some analysis is required. Our first observation is that the linearized equations contain a negative feedback loop, and thus one may anticipate that oscillations could exist for appropriate parameter values. Next we show that excitability and the existence of a threshold can be understood by considering a certain two-dimensional fast subsystem of the four-dimensional system. In the second subsection we present some numerical solutions to (10) using the same parameters as in the preceding section, except for the adenylate cyclase velocity. These solutions show good qualitative and quantitative agreement with the experimental observations on oscillations in suspensions. We also investigate the effects of changing some of the enzyme parameters in the model. In the third subsection we examine the effects of varying some parameters that may be experimentally controllable. Our purpose in investigating parameter dependence is twofold. Firstly, we intend to show that developmentally controlled variations in the velocity of adenylate cyclase (V_1) and the velocity of extracellular membrane-bound phosphodiesterase (V_{PO}) can account for the transition from relay competence or excitability to autonomous oscillatory pacemaker behaviour that is observed experimentally. Secondly, the parameters such as the density of the cells in suspension (ρ) and the total calcium present in the experiment ($\bar{x}_6$) are under experimental control, and thus the parametric studies may suggest new experiments designed to test the model.

PHILOSOPHICAL TRANSACTIONS OF THE ROYAL SOCIETY B BIOLOGICAL SCIENCES

4.1. *Heuristics on the origin of the oscillations*

A useful technique for understanding the mechanism underlying periodic behaviour is the graph of the control structure in the differential equations (Othmer 1976). In such a graph the nodes represent the chemical species in the model, and an edge is drawn from node ***a*** to ***b*** if species ***a*** appears in the differential equation for species ***b***. The weight associated with this edge is the corresponding entry in the Jacobian at a steady state. A feedback loop in such a graph is a closed circuit in the graph, the weight on a loop is the value of the product of the weights for the steps in the circuit, and its sign is the sign of this product. For low-dimensional systems (less than five variables) negative feedback loops tend to produce oscillations, whereas positive feedback loops tend to produce multiple steady states (see Othmer (1976) for a more precise formulation of these facts). In figure 7 we show the graph associated with equations (10). This contains a positive feedback loop of length two (between intracellular and extracellular cyclic AMP), a negative feedback loop of length three (between extracellular cyclic AMP, intracellular calcium and intracellular cyclic AMP) and a positive feedback loop of length three containing sequestered calcium. Because all species are self-damping the positive feedback loop of length two tends to produce multiple steady states, as does the positive feedback loop of length three. However, the negative feedback loop may destabilize the steady state via growing oscillations if the weight on this loop is sufficiently large in magnitude. This occurs, for instance, when the sensitivity of adenylate cyclase to intracellular calcium is sufficiently large and the remaining sensitivities have the proper magnitude. We show later that this is possible for suitable ranges of the parameters.

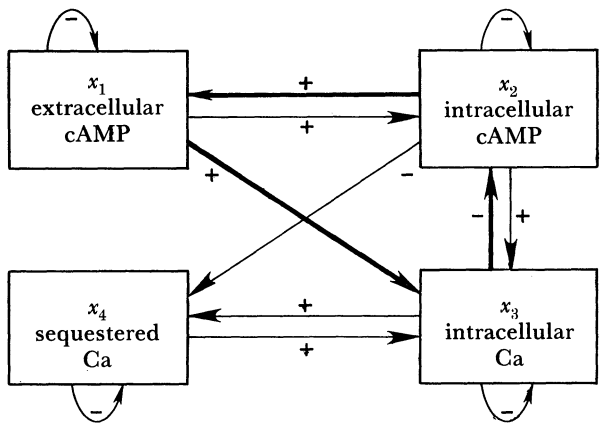

FIGURE 7. Graph of the control structure of the model given by (10). The thick lines in the diagram represent the negative feedback loop of length three that leads to the oscillatory instability of the steady state.

To understand the origin of excitability and the transition from a stable, excitable system to one supporting autonomous oscillations, we consider two separate projections of the four-dimensional phase space for (10) onto two-dimensional manifolds. Firstly, because we want to study the sensitivity of the steady state to perturbations in extracellular cyclic AMP (x_1), and because this is controlled in part by slow variations in intracellular calcium (x_3), we project onto the manifold defined by $dx_2/d\tau = 0$ and $dx_4/d\tau = 0$. This manifold is then parametrized by x_1 and x_3. It will become clear later that the $dx_2/d\tau$ equation is not singularly perturbed, but as we shall see this projection can still give insight into the dynamics of the full system.

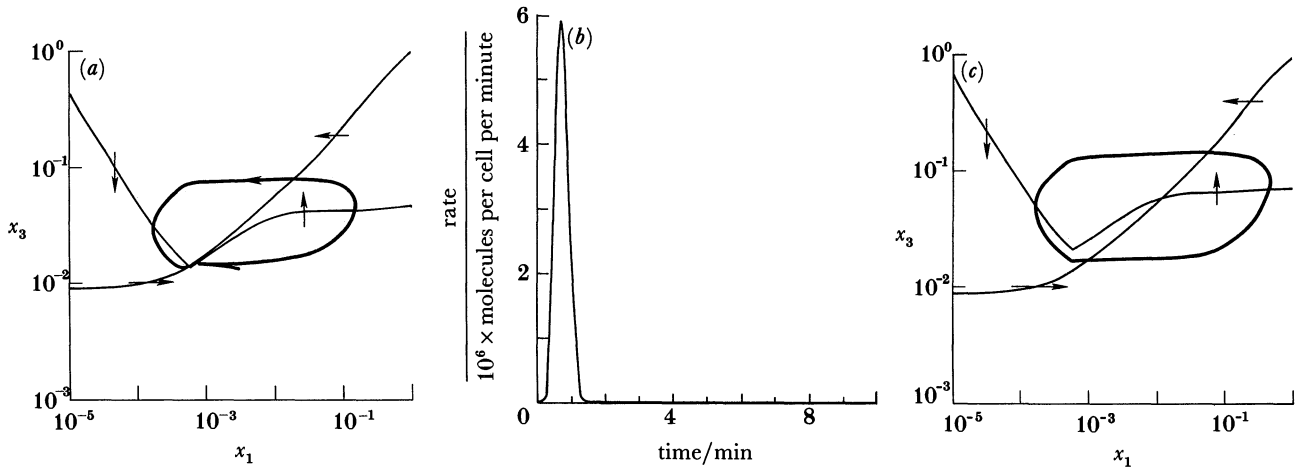

FIGURE 8. A section of phase space on the manifold defined by $dx_2/d\tau = 0$ and $dx_4/d\tau = 0$. The arrows on the nullclines show the directions of the vector field along the nullcline on this section. The trajectories shown are the x_1 and x_3 components of the full solution. Parameter values are as given in table 3, with the exception of V_1. (*a*) $V_1 = 0.13$. The steady state is close to the minimum in the $dx_1/d\tau = 0$ curve. Although the steady state is still stable, a small increase in x_1 leads to a large amplification of the disturbance. The system is excitable or relay competent. Note that x_1 decreases initially, which is reflected in the secretion rate shown in (*b*). (*b*) A graph of the cyclic AMP secretion rate against time for the trajectory shown in (*a*). The transient rise in the intracellular cyclic AMP concentration after stimulation results in a rapid transient rise in the secretion rate. This is the relay response. (*c*) $V_1 = 0.2$. Now the steady state is unstable and a stable limit cycle exists.

Figure 8 shows the projected phase space for two different values of V_1, which scales the velocity of adenylate cyclase. If V_1 is small enough, the nullclines cross to the left of the minimum in $dx_1/d\tau = 0$, and computations of the eigenvalues of the Jacobian at the steady state show that the steady state is stable. When V_1 is very small the steady state lies far above the turning point in the $dx_1/d\tau$ nullcline and a very large relative increase in x_1 is needed to produce a response in which the perturbation in x_1 is ultimately amplified. In fact, because a perturbation in x_1 moves off the $dx_2/d\tau = dx_4/d\tau = 0$ manifold, x_1 must be increased well beyond the $dx_1/d\tau$ nullcline before the system will amplify x_1. As V_1 increases the point of intersection of the nullclines approaches the minimum in the $dx_1/d\tau$ nullcline (figure 8*a*). The steady state is still stable, but now a small relative increase in x_1 will elicit a large transient pulse of x_1 before the return to steady state, and the system is said to be excitable. The corresponding pulse of cyclic AMP that is released is shown in figure 8*b*.

However, figure 8*a* also shows that x_1 decreases initially, even though it grows eventually. This is evidently not possible in a simple system such as the Fitzhugh–Nagumo equations, and to understand this we consider a reduction that isolates a relatively fast two-dimensional subsystem in the model. The computations done in §2 with the standard parameters show that the sequestered calcium equilibrates rapidly with the free calcium, and to simplify the analysis we assume that x_4 is at steady state. This reduces (10) to a three-dimensional system. Moreover, x_1 and x_2 initially vary on a time scale that is fast compared with x_3, although the time scales are not sufficiently separated to apply singular perturbation throughout the course of a response.

Suppose that V_1 is at a value appropriate for the perfusion experiments. Then one sees from figure 8*a* that there is a unique steady state, and this steady state can be shown to be stable. If the system is at this steady state and x_1 is increased rapidly, the initial response of the system

is governed by the behaviour of the fast x_1–x_2 subsystem with x_3 fixed at the steady-state value. Because the interaction between x_1 and x_2 is via a positive feedback loop (see figure 7), the earlier discussion suggests that there may be multiple steady states in this subsystem. This is indeed the case, as is seen in the x_1–x_2 phase plane shown in figure 9*a*.

The steady state with the lowest value of x_1, which corresponds to the steady state for the full system, is stable. The intermediate steady state is a saddle point and the upper steady state is stable. The unstable manifold of the saddle point defines the threshold stimulation needed to elicit a large response in x_1. If the initial condition is such that x_1 lies to the left of this manifold the response is subthreshold and there is no amplification in x_1, whereas if the initial point lies just to the right of this manifold there is (eventually) a large amplification in x_1. Note that the schematic in figure 9*a* shows that it is possible for x_1 to decrease initially before a pulse is generated, which accounts for the initial behaviour shown in figure 8*a*. The fact that the unstable rest point in figure 9*a* is close to the lower steady state means that a small increase in x_1 will elicit a large response, i.e. the system is excitable.

If calcium is regarded as a parameter and is increased from its steady-state value, the upper stable and the unstable steady states of the x_1–x_2 subsystem eventually coalesce and disappear,

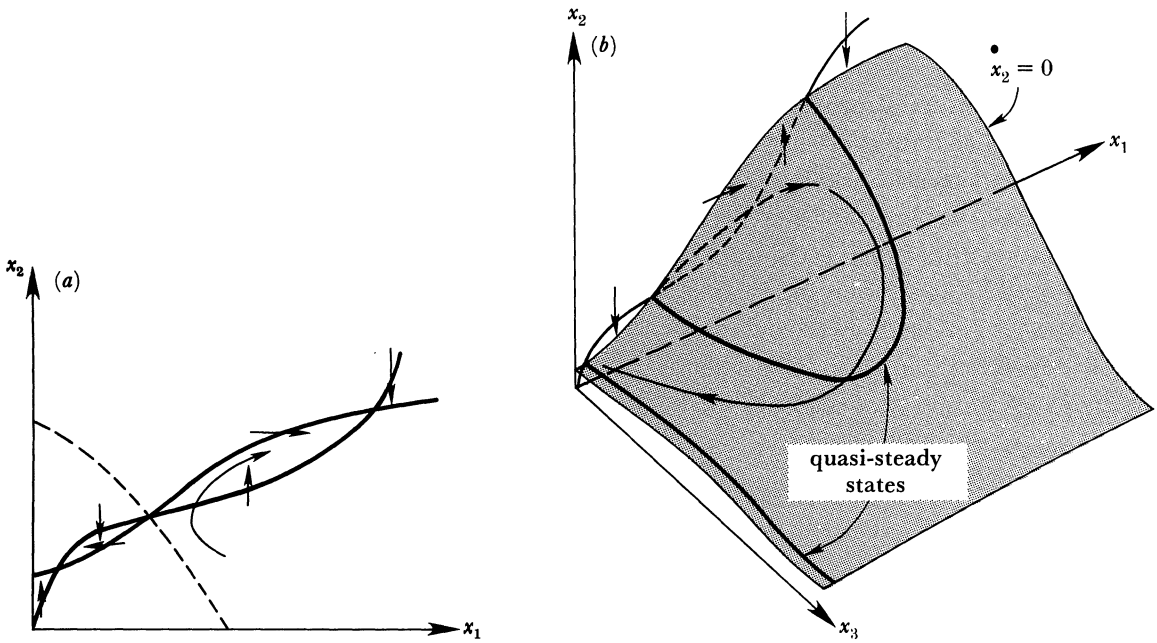

FIGURE 9. The x_1–x_2 subsystem. (*a*) A sketch of the nullclines $dx_1/d\tau = 0$ and $dx_2/d\tau = 0$ with x_3 (cytoplasmic calcium) fixed at steady state. There are three steady states in this subsystem, the left-most of which is the stable steady state of the full system (for clarity the distance between the left two steady states has been exaggerated). The thick arrows show the direction of flow at each nullcline, and the longer thin arrow shows the early time behaviour of a solution similar to that shown in figure 8*a*. The relay response is initiated by perturbing x_1 from steady state across the dashed line. The resulting solution can first move towards the intermediate steady state, but eventually it approaches the upper steady state. The broken line is the unstable manifold of the intermediate steady state. It marks the threshold for amplification of a perturbation from the lowest steady state. (*b*) A schematic of three dimensional phase space showing the development of a relay response. For simplicity the sequestered calcium compartment has been ignored. A perturbation of sufficient magnitude in x_1 from the steady state results in a fast movement towards the upper steady state in the x_1–x_2 plane as discussed in (*a*). The solution then tracks the upper quasi-steady-state as intracellular calcium increases. When x_3 is large enough the upper steady state ceases to exist, and the solution jumps to the lower quasi-steady-state and returns slowly to the steady state of the system. This picture is accurate if the x_1 and x_2 equations are singularly perturbed, and gives a qualitative understanding of excitability for the parameters used in this paper.

PHILOSOPHICAL TRANSACTIONS OF THE ROYAL SOCIETY B BIOLOGICAL SCIENCES

and only the lower steady state remains. If there was a large difference between the time scale of the x_1–x_2 system and the calcium response, the phase point would move to a neighbourhood of the upper steady state after a superthreshold stimulus and slowly track the slow manifold obtained by a singular perturbation of the x_1–x_2 subsystem. In reality the time scales are not separated sufficiently to apply this kind of argument throughout the response, because calcium begins to rise significantly before the trajectory reaches a small neighbourhood of the upper steady state. However, the foregoing analysis does provide a qualitative understanding of the origin of the threshold and of the early dynamics following stimulation. A composite sketch of the response in three dimensions is shown in figure 9*b*.

The transition from excitability to autonomous oscillations can be understood with reference to figure 8. As V_1 is increased beyond the value for relay, it is seen in figure 8*b* that the steady state moves to the right of the knee in the $dx_1/d\tau$ nullcline, and one can show that it becomes unstable. The numerical computations described later show that there is a Hopf bifurcation at this point, and periodic solutions emerge from the steady state.

We can gain further understanding of the oscillations by using the response surface discussed in the previous section. Figure 10 shows the surface for (11), on which is superimposed a curve that represents the extracellular cyclic AMP and cytosol calcium components of a periodic solution. It can be seen that the oscillation is divided into essentially three portions, two of which are fast and one of which is slow. The first phase is a slow fall in the cytosol calcium concentration at an approximately fixed low level of extracellular cyclic AMP. In this phase most of the adenylate cyclase is deactivated, although as cytoplasmic levels of calcium fall the level of deactivation of adenylate cyclase falls. It is this slight rise in adenylate cyclase activity that initiates the first fast phase in the oscillation, in which the extracellular cyclic AMP concentration rises rapidly, together with a slower rise in intracellular calcium. Because of the positive feedback between intracellular and extracellular cyclic AMP, as extracellular cyclic AMP rises it also increases adenylate cyclase activity, thereby increasing the intracellular cyclic AMP concentration. This phase is terminated by the concurrent rise in the cytoplasmic calcium concentration, because of the increasing permeability of the cell membrane to calcium.

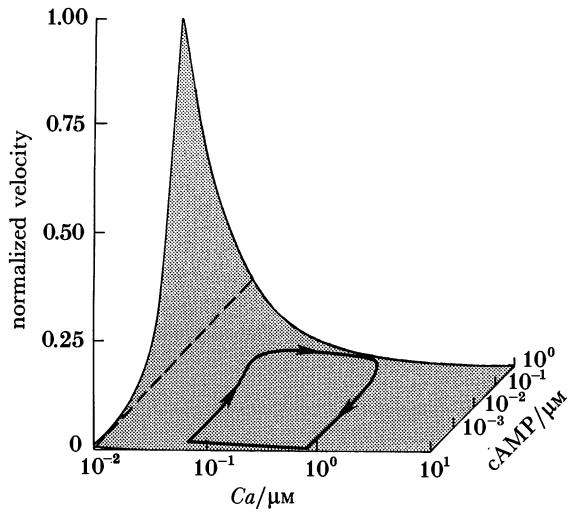

FIGURE 10. A response surface for (11) with a superimposed trajectory of a periodic solution, the latter computed using parameters in table 3, except that $V_1 = 0.5$ (see figure 3 for an explanation of the surface).

PHILOSOPHICAL TRANSACTIONS OF THE ROYAL SOCIETY B BIOLOGICAL SCIENCES

This leads to the third phase of the oscillation, in which extracellular cyclic AMP is rapidly hydrolysed by extracellular phosphodiesterase. In this phase the cytoplasmic calcium concentration also peaks and begins to decrease, thereby completing the cycle.

4.2. *The effect of changes in the major enzymes*

In this and the following subsection we discuss the dependence of the solutions of (10) on parameters that vary with developmental age or that can be controlled experimentally. The reader can consult (11) and §3 for the effects of parameters on the dynamics of the model when extracellular cyclic AMP is clamped. We present some bifurcation diagrams computed for selected parameter values, using the bifurcation analysis package AUTO developed by Doedel (Doedel & Kernevez 1986). Unless stated otherwise, all parameters except the ones being varied have the values given in table 3, which are those used in the relay/adaptation computations.

First we consider the effects of increases in adenylate cyclase velocity (V_1) and the velocity of extracellular membrane bound phosphodiesterase (V_{PO}). The experimental observations are as follows.

1. As was discussed in the Introduction, cells become relay competent after a period of starvation. During this period there is a rise in the levels of intra- and extracellular cyclic AMP (Brenner 1978; Abe & Yanagisawa 1983) and in the activity of adenylate cyclase (Klein 1976; Klein & Darmon 1977; Loomis 1979). Whether this is due to an increase in the overall amount of enzyme present or to an increased sensitivity to stimulus is not known, but Loomis (1979) argues that the increase in activity is due to newly made enzyme. The latter possibility would lead to an increase in V_1 in our model. Extracellular phosphodiesterase activity also increases during this time (Abe & Yanagisawa 1983; Brenner 1978).

2. After about eight hours of starvation, suspensions of cells start to show periodic behaviour (Raman *et al.* 1976) that is manifested as oscillations in the concentration of cyclic AMP and calcium (see references in the Introduction). The levels of extracellular phosphodiesterase, cyclic AMP and adenylate cyclase activity peak at about this time (Klein & Darmon 1977; Brenner 1978; Loomis 1979; Abe & Yanagisawa 1983). The peak in free phosphodiesterase is less apparent than for the membrane-bound form, and Brenner (1978) argues that the cell associated form is more important for cyclic AMP hydrolysis, at least during aggregation.

As we have seen previously, at small values of V_1 there is a unique steady state, which is stable and at which the system is inexcitable. As V_1 is increased the system becomes excitable, and if V_1 increases still further the stable steady state becomes unstable and gives rise to a branch of stable periodic solutions. If V_1 is made sufficiently large the periodic solution vanishes and the only attractor is a stable steady state. A bifurcation diagram showing how the periodic solutions emerge via Hopf bifurcations is given in figure 11. Note that at some values of V_1 there are two possible stable periodic solutions, and at other values of V_1 a stable steady state and a stable periodic solution coexist. Here and hereafter we use $\alpha = 1$ in (10) to avoid certain numerical difficulties in the bifurcation calculations. Separate numerical experiments show that the results are essentially independent of α for $\alpha \in [0.85, 1]$.

The time behaviour of solutions at selected values of V_1 is shown in figure 12. The results are displayed after the equations have been integrated for the equivalent of 25 min to ensure that the transient behaviour has decayed. All the parameter values except for V_1 are given in table

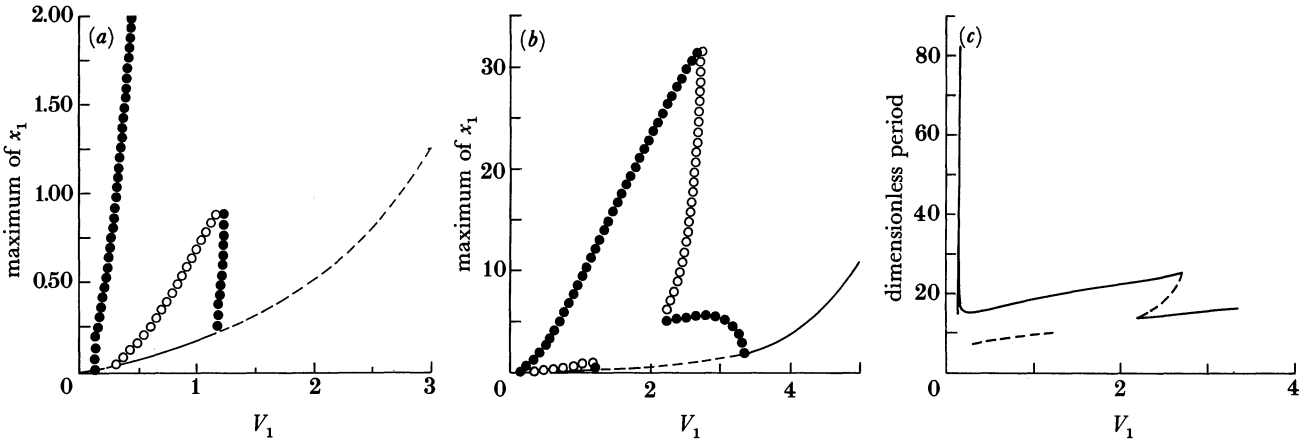

FIGURE 11. The variation of the solution with variations in V_1. These figures show how the solution set changes as the parameter V_1, which multiplies the adenylate cyclase velocity, is varied. As discussed in the text, this parameter may change with the developmental age of the cell. All parameters except V_1 are at the values given in table 3. (*a*) The maximum of x_1 as a function of V_1 for small V_1. The thin lines represent steady states of the system (solid: stable; broken: unstable), and the circles represent periodic solutions (open: unstable; filled: stable). At a steady state the ordinate represents the x_1-component of the solution; on a periodic solution it represents the maximum value of x_1 on the periodic orbit. Beginning at low V_1 there is a single stable steady state, but as V_1 increases there is a Hopf bifurcation at which a branch of stable periodic solutions emerges. This branch bifurcates at $V_1 \approx 0.13$, corresponding to the transition from excitable to periodic behaviour discussed in the context of figure 8. As V_1 increases further the steady state regains stability and a different, unstable, branch of periodic solutions emerges. The steady state loses stability again at $V_1 \approx 1.20$, and another stable periodic solution emerges. To convert the ordinate to dimensional extracellular cyclic AMP concentrations in micromolar units, multiply the values given by 0.5. (*b*) The global diagram corresponding to (*a*). Note that there are two intervals in which two distinct stable periodic solutions exist. (*c*) The global behaviour of the dimensionless period of the different periodic solutions as a function of V_1. To convert to minutes divide by 2. Note that whenever there are two distinct stable periodic solutions they have a different period. Note also that the stable periodic solution that emerges at the first bifurcation point has a very long period, which is explained by the fact that there is a very slow buildup of cyclic AMP close to the transition from excitability to periodic behaviour.

3 and are the same as used in modelling the perfusion experiments. That the calcium parameters are unchanged is in accordance with the observations of Europe-Finner & Newell (1985). Parameter values for the external compartment are discussed in Appendix 1.

The results for $V_1 = 0.5$ in figure 12 are in good agreement with the experimental results. The period and amplitude of the intracellular and extracellular cyclic AMP concentrations and the half-widths of the peaks are in the range of the experimental observations, but the half-width of the intracellular cyclic AMP peak is larger than for extracellular cyclic AMP, in contrast with the experimental results. As we shall see in §5, the latter discrepancy can be explained by assuming that the suspensions are not perfectly mixed, and allowing for the formation of small aggregates of cells within the suspension. In addition, the experimental results concern large numbers of cells, and slight asynchronies will tend to broaden both experimentally observed intracellular and extracellular cyclic AMP peaks.

To understand how changes in the activity of the extracellular phosphodiesterases affect the range of V_1 over which oscillations exist, we have computed the locus of Hopf bifurcation points in (V_{PO}, V_1) and (V_{PE}, V_1) space. From these we can predict how a cell can progress from quiescent behaviour through excitability to periodic behaviour as the activity of different enzymes changes. Figure 13 shows the results of these computations. As we know from the results given in figure 11, periodic solutions exist over the range of parameters for which the

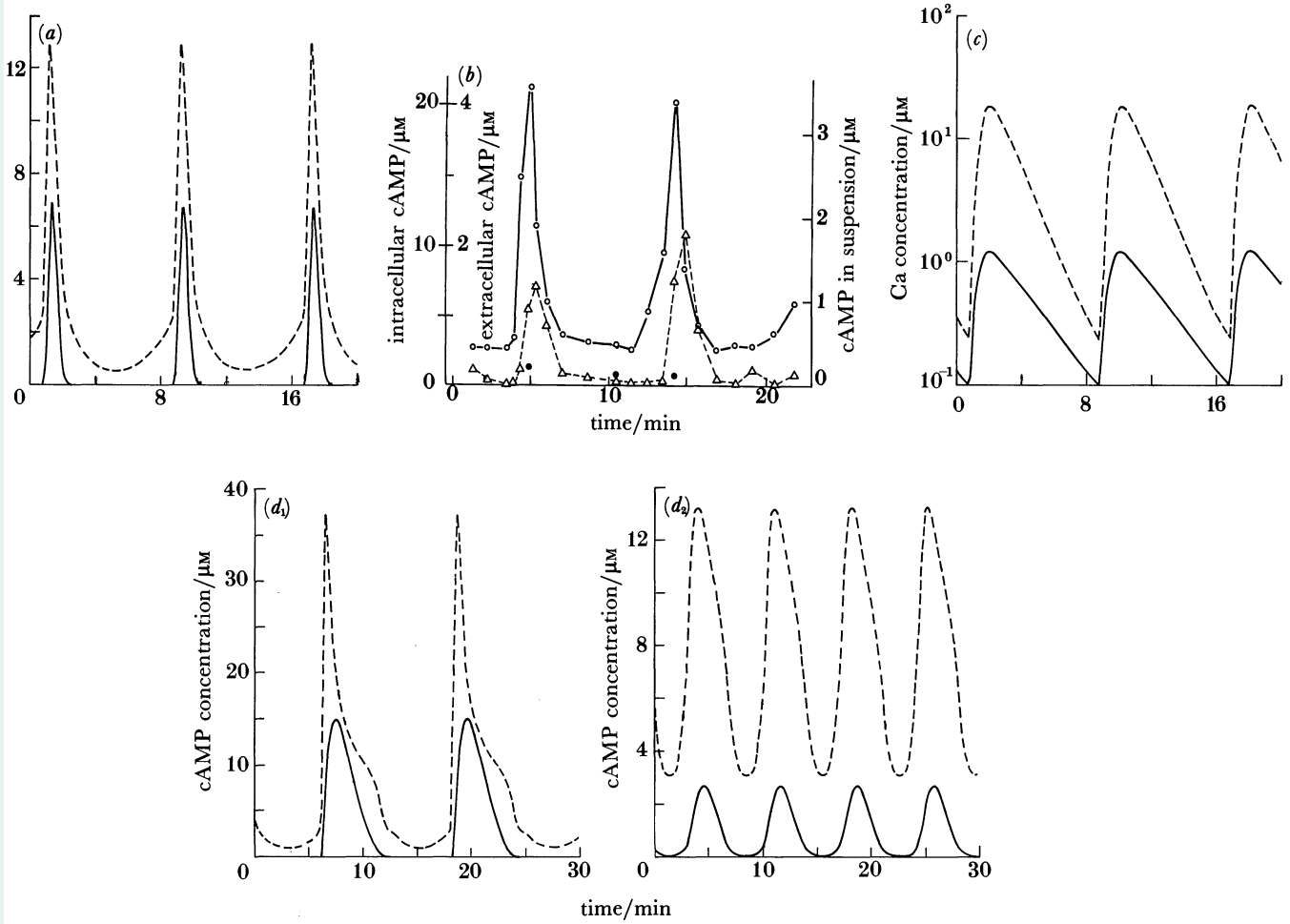

FIGURE 12. The temporal variation of the components of the periodic solutions for several values of V_1. The values of the remaining parameter values are given in table 3. (*a*) $V_1 = 0.5$. This value is chosen for comparison with the experimental results. Both intracellular and extracellular cyclic AMP are shown, and these plots should be compared with the experimental results shown in (*b*). Solid curve: extracellular concentration times five; broken curve: intracellular concentration. (*b*) Experimental measurements of intracellular (○) and extracellular (△) cyclic AMP oscillations (redrawn from figure 2 of Gerisch & Wick (1975)). (*c*) The calcium concentrations for the solutions shown in (*a*). Solid curve: cytosol calcium; broken curve: sequestered calcium. (*d*) $V_1 = 2.5$. The cyclic AMP concentrations on the two distinct periodic solutions (cf. figure 11*b*). Solid curve: extracellular concentration; broken curve: intracellular concentration. A comparison of the cyclic AMP curves shown and the corresponding curves of calcium concentration (not shown) shows that there is a very large difference in the amplitude of the cyclic AMP oscillation, but relatively little difference in the peak values of cytosol calcium (cf. also figure 11*b*).

steady state is unstable, and frequently over a larger range. Thus the regions of instability depicted in figure 13 and the following figures provide a conservative estimate of where periodic behaviour will be observed. Suppose that V_1 and V_{PO} both increase as development proceeds, as is suggested by the experimental results. From figure 13*a* we see that the transition from quiescent behaviour to relay competence can be explained by an increase in V_1. If the parameter point (V_1, V_{PO}) for a suspension of cells lies to the left of the vertical line $V_1 \approx 0.13$ in figure 13*a* the suspension is not oscillatory, and the cells secrete cyclic AMP at a low basal level. If V_1 and V_{PO} then increase so that the left-most curve of Hopf points is approached, the

PHILOSOPHICAL TRANSACTIONS OF THE ROYAL SOCIETY B BIOLOGICAL SCIENCES

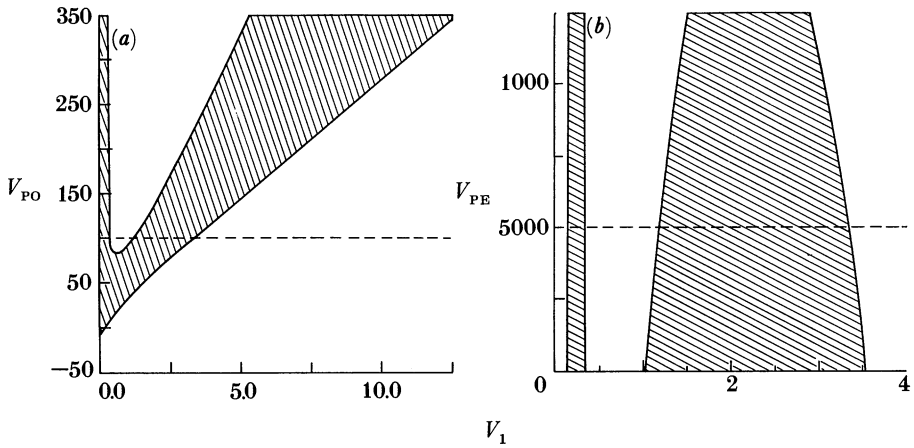

FIGURE 13. The effects of changing extracellular phosphodiesterase velocities. In each diagram the value of the phosphodiesterase velocity used in the previous simulations is shown by a broken line, and the hatching denotes the regions of parameter space in which the steady state is unstable. (*a*) The (V_1, V_{PO}) parameter plane showing the locus of Hopf bifurcation points (i.e. the points at which the steady state loses stability because of growing oscillations). The location of the first Hopf point (not shown) for increasing V_1 at fixed V_{PO}, which corresponds to the transition from excitability to periodicity, occurs at $V_1 \approx 0.135$ and is essentially independent of V_{PO}. This diagram depicts how changes in the activity of membrane-bound phosphodiesterase affect the range of V_1 for which periodic solutions exist. Both parameters increase with developmental age, and it is easy to imagine a path in the plane along which both V_1 and V_{PO} increase, and on which the stable attractor in the model changes from a single steady state to a periodic solution and back to a steady state. (*b*) A graph in the (V_1, V_{PE}) parameter plane of the locus of Hopf points. This diagram shows the effects of changing extracellular free phosphodiesterase activity. For the range of activity shown the line of Hopf points at lowest V_1 is almost vertical, which indicates that changes in V_{PE} have little effect on the onset of periodicity as V_1 increases.

system will become more and more sensitive to stimulus, but will still remain at a steady state corresponding to relay competence. As the parameter point (V_1, V_{PO}) crosses the left-most locus of Hopf bifurcation points and moves into the region in which the steady state is unstable (marked by hatching in the figure), periodic oscillations will appear. If the point (V_1, V_{PO}) traverses the region of instability to sufficiently large values of V_1 and V_{PO}, the steady state regains stability and the periodic solutions disappear. Similar computations varying V_{PE} show that changes in the velocity of the free extracellular phosphodiesterase have less effect on the transitions from stable steady states to periodic solutions than do changes in V_{PO}, as is shown in figure 13*b*. Increasing V_1 at fixed V_{PE} always results in four Hopf bifurcation points, and the location of the lower pair of Hopf points is essentially independent of V_{PE} for experimentally reasonable values of the parameters V_1 and V_{PE}.

4.3. *Dependence of the solutions on cell density and total calcium*

The two parameters most easily manipulated experimentally are the cell density and the total calcium in a suspension. These are reflected in the dimensionless parameters ρ and $\bar{x}_6$, respectively. We discuss density effects first. If ρ is small there are few cells present and one would not expect oscillations in a suspension. This is difficult to prove in general for (10), but because $R_c \approx 1$ the sequestration compartment equilibrates rapidly, and to a good approximation (10) can be reduced to a three-dimensional system for x_1, x_2 and x_3. When ρ is small enough $x_1(\tau)$ is slowly varying, and the initial evolution is governed by the solution of the (x_2, x_3) subsystem. However, it is easy to see that this two-dimensional system has a unique stable rest point for any fixed $x_1 \geqslant 0$. Thus for sufficiently small ρ the rest point in the full system

is unique and stable. On the other hand, we know from results given earlier that if ρ is large enough the steady state may be unstable and stable periodic solutions can exist. Figure 14 shows the computed loci of Hopf bifurcation points in the (V_1, ρ) plane. If V_1 is fixed at a sufficiently large value and ρ is increased from zero the following transitions are observed. There is a single stable steady state at low values of ρ, and this loses stability and periodic solutions emerge when ρ is large enough. Because V_1 varies with developmental age, figure 14 suggests that the critical density at which a suspension of cells will undergo spontaneous oscillation will vary with age. These figures also suggest how clustering in a non-uniform suspension of cells could lead to precocious oscillations. Regions of locally high density could begin to oscillate while regions of low density remain quiescent, although one expects the latter may be entrained by the former if the amplitude of oscillation is large enough. This is discussed further in the next section.

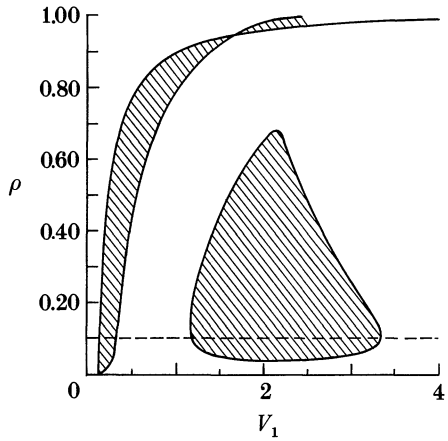

FIGURE 14. The regions of instability of the steady state in the (V_1, ρ) plane. The curves shown are the loci of Hopf bifurcation points. The broken line marks the value of ρ used in previous computations, and the hatched region shows where the steady state is unstable. For a wide range of density ρ the system can progress from a stable steady state to periodicity by an increase in V_1. Note that the second interval of instability in V_1 at fixed ρ disappears at sufficiently high densities. If ρ is too small periodic solutions do not exist for any value of V_1.

Next we study the effect of variations in the total amount of calcium in a suspension. In figure 15 we show the regions of instability in the $(V_1, \bar{x}_6)$ plane. As in previous two-parameter diagrams, the boundaries of the hatched regions are the loci on which Hopf bifurcations occur. We see in figure 15 that at low levels of total calcium $(\bar{x}_6)$ there is a stable steady state, and as $\bar{x}_6$ increases at a fixed value of V_1 a periodic solution emerges via a Hopf bifurcation. At intermediate values of total calcium the steady state is stable, but of course there may also be a large-amplitude periodic solution that coexists with the stable steady state. At larger values of calcium the steady state is again unstable over an interval of calcium concentrations.

The dependence of the solutions on $\bar{x}_6$ for fixed $V_1 = 0.5$ is shown in figure 16. The solutions at $\bar{x}_6 = 1.0$ are identical with those at $V_1 = 0.5$ in figure 11. Note that in figure 16 there is an interval of $\bar{x}_6$ in which there are two stable periodic solutions that coexist. The cyclic AMP concentration computed for $\bar{x}_6$ in this interval are shown in figure 17. One of these solutions has a large amplitude in both cyclic AMP and cytosol calcium, whereas the other has a much smaller amplitude in these components. As we noted in the Introduction, Bumann *et al.* (1986) discovered two types of external calcium oscillation, a large amplitude spike-shaped

PHILOSOPHICAL TRANSACTIONS OF THE ROYAL SOCIETY B BIOLOGICAL SCIENCES

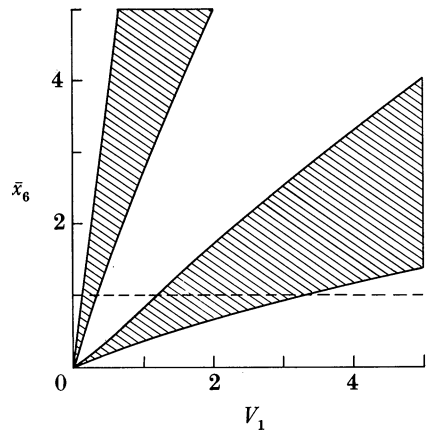

FIGURE 15. The regions of instability of the steady state in the $(V_1, \bar{x}_6)$ plane. The steady state is unstable in the hatched regions. The broken line marks the value of the total calcium $\bar{x}_6$ used in the previous computations.

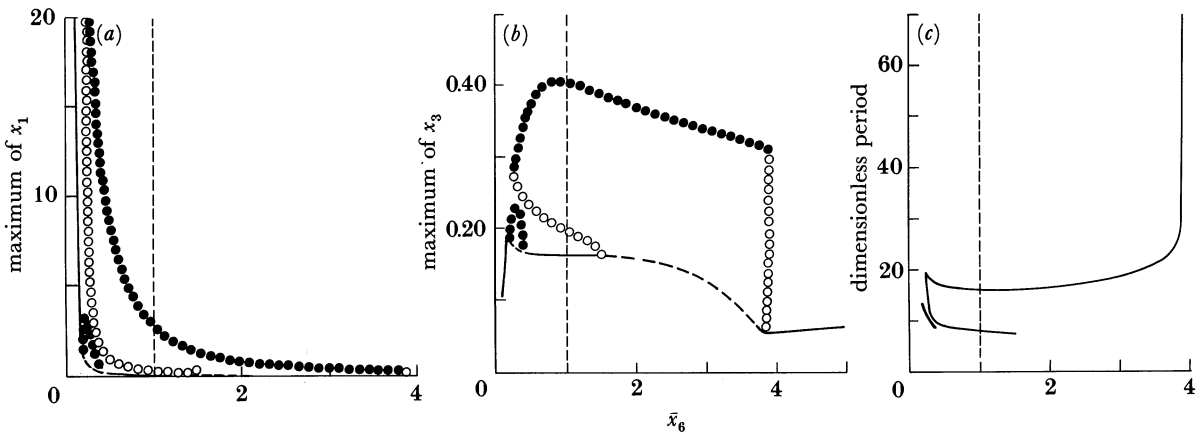

FIGURE 16. The dependence of the steady state and the periodic solutions on the total calcium concentration. The broken vertical line marks the value of $\bar{x}_6$ used in the previous computations. See figure 11 for an explanation of the symbols and the scale factors for the dimensionless variables. To convert $\bar{x}_6$ to micromolar units multiply by three. (*a*) The dependence of the maximum dimensionless extracellular cyclic AMP concentration on $\bar{x}_6$. (*b*) The dependence of the maximum dimensionless cytosol calcium concentration on $\bar{x}_6$. Note that for a range of $\bar{x}_6$ there are two stable periodic solutions that coexist. The domain of attraction of the large-amplitude solution is large compared with that of the small-amplitude solution. Also note that the maximum cytosol calcium concentration on the large-amplitude solution is relatively insensitive to changes in the total calcium present, whereas the cyclic AMP concentration depends very strongly on the total calcium concentration. (*c*) The period of the periodic solutions as a function of $\bar{x}_6$. Note that the period of the large-amplitude solution is approximately 10 min over a wide range of the total calcium concentration. As noted in the text, this value is consistent with numerous experimental observations.

oscillation associated with cyclic AMP oscillations, and a smaller-amplitude sinusoidal oscillation not accompanied by a measurable cyclic AMP oscillation. Our results show that the small-amplitude, nearly sinusoidal oscillations in calcium are accompanied by relatively small amplitude cyclic AMP oscillations. Whether or not these solutions are related to those observed by Bumann *et al.* is an open question.

PHILOSOPHICAL TRANSACTIONS OF THE ROYAL SOCIETY B BIOLOGICAL SCIENCES

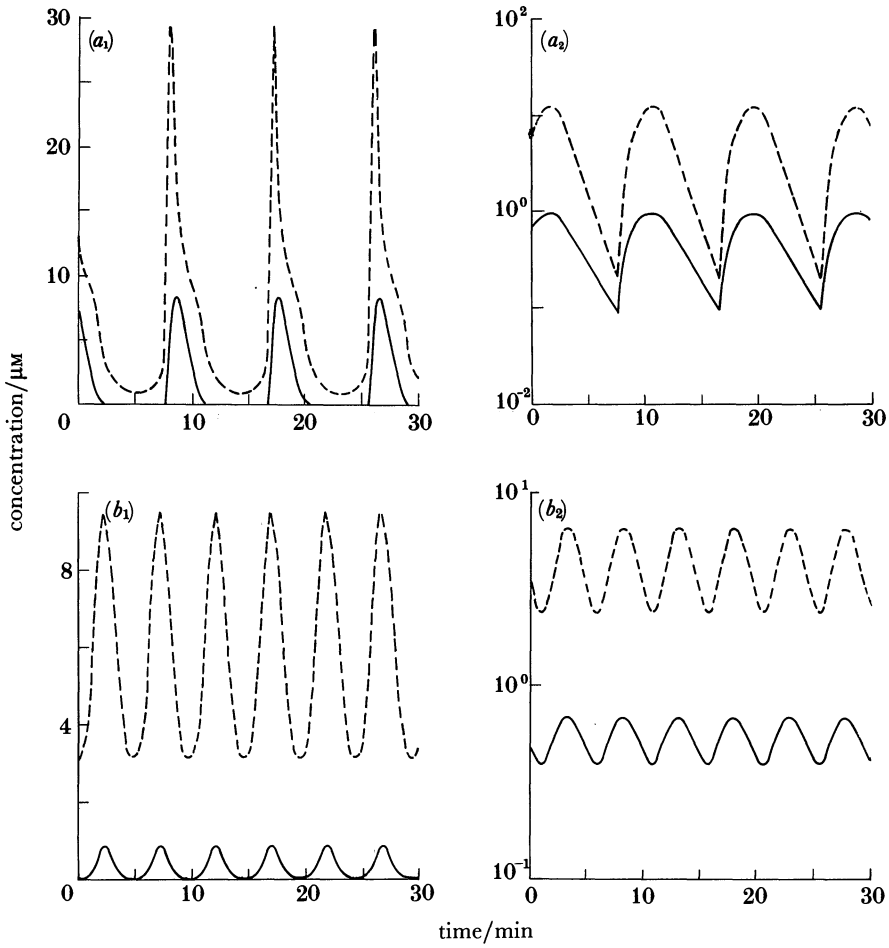

FIGURE 17. The temporal variation of the cyclic AMP and calcium concentrations on the periodic solutions that coexist at $\bar{x}_6 = 0.3$. (*a*) The cyclic AMP (a_1) and calcium (a_2) concentrations on the large-amplitude solution. Solid lines: extracellular cyclic AMP and cytosol calcium; broken lines: intracellular cyclic AMP and sequestered calcium. (*b*) Same as (*a*), but for the small-amplitude solution.

5. GENERALIZATIONS OF THE BASIC MODEL

In the previous section we demonstrated that the solutions of the equations that govern the dynamics of the basic model are in good agreement with the experimental results on the amplitude of the cyclic AMP oscillations and the period of these oscillations. There are, however, several biologically realistic modifications of the basic model that should be tested. These modifications are (i) incorporation of aggregation of cells into small clusters, (ii) allowance for heterogeneity in the developmental age or other physiological characteristics of the cells, and (iii) allowance for time delays in certain control steps. The last modification is one way of examining the effects of longer biochemical pathways in the control steps. In the following three subsections we investigate each of these three modifications separately, and show how these modifications improve the response. We do not introduce these simultaneously, but the reader can deduce the effect of doing this from the results we present.

PHILOSOPHICAL TRANSACTIONS OF THE ROYAL SOCIETY B BIOLOGICAL SCIENCES

5.1. *The effects of aggregation in suspensions*

First we allow for the formation of small aggregates in the suspension. Suspensions of *Dictyostelium* are usually stirred by bubbling oxygen through the fluid (Gerisch *et al.* 1975), and although this stirring certainly prevents the formation of large aggregates of cells, it may not prevent the formation of small aggregates of cells. Such small aggregates may have a major effect on the dynamics of cell suspensions (P. N. Devreotes, personal communication; Weiger *et al.* 1984). To investigate the effects of aggregation on the dynamics, we modify the external cyclic AMP and external calcium equations in (10) to incorporate this effect.

We assume that the N cells in a suspension form aggregates containing n cells each, and that there is a finite resistance to transport between the fluid trapped in an aggregate and the fluid outside an aggregate. Both the fluid within an aggregate and the exterior fluid are homogeneous, but the concentrations of cyclic AMP and calcium may be different in the two compartments. Let C_0 and Ca_0 be the concentrations of cyclic AMP and calcium within each aggregate, and let C_0' and Ca_0' be the concentration of cyclic AMP and calcium outside the aggregates in the cell-free fluid. We define $x_1 = C_0/K_m$, $x_6 = Ca_0/K_{seq}$, $x_7 = C_0'/K_m$, and $x_8 = Ca_0'/K_{seq}$, and then obtain the following differential equations governing the behaviour of the external variables.

$$\left.\begin{aligned}
\frac{dx_1}{d\tau} &= \frac{R_c}{\epsilon}\left(R_H f_2(x_2) - V_{PO}\left(\frac{x_1^\alpha}{1+x_1^\alpha}\right) + HR_H(R_H x_2 - x_1) + K_{CP}(x_7 - x_1)\right) \\
&\quad - R_c\left(\frac{\rho}{1-\rho}\right) V_{PE}\left(\frac{x_1}{R_e + x_1}\right) \\
\frac{dx_6}{d\tau} &= \frac{R_c}{\epsilon}\left(K_{Ca}(x_8 - x_6) - \left(R_1(x_1)\left(\frac{x_6}{K_F + x_6}\right) - V_{PU}\left(\frac{x_3^{q_4}}{K_{PU}^{q_4} + x_3^{q_4}}\right)\right)\right) \\
\frac{dx_7}{d\tau} &= R_c\left\{\frac{\rho K_{CP}}{1-(1+\epsilon)\rho}(x_1 - x_7) - \left(\frac{\rho}{1-\rho}\right) V_{PE}\left(\frac{x_7}{R_e + x_7}\right)\right\} \\
x_8 &= \left(\frac{1}{1-(1+\epsilon)\rho}\right)(\bar{x}_6 - R_c\rho x_3 - (1-R_c)\rho x_4 - \rho\epsilon x_6)
\end{aligned}\right\} \tag{18}$$

In these equations the final equation is the conservation condition for calcium. K_{CP} and K_{Ca} are positive constants that are defined in table 2, and ϵ is the ratio of free volume (extracellular fluid volume) to total cell volume in an aggregate. The quantity $(1+\epsilon)\rho$ is the fraction of the total volume contained in aggregates, which must be less than one. As before, we have also assumed that the vesicle compartment equilibrates rapidly. Note that these equations reduce to the model studied in §4 if the coefficients K_{CP} and K_{Ca} are large. In that case the transport of calcium and cyclic AMP in and out of the aggregates is so rapid that differences between aggregate and bulk concentrations can be ignored.

The choice of parameters ϵ, K_{Ca} and K_{CP} is difficult because nothing is known about the geometry of the aggregates. If we assume an aggregate of close packed spheres, ϵ is approximately 0.9, and this is the value we use in the simulation shown in figure 18. The flux constants K_{Ca} and K_{CP} are much more difficult to estimate. An order of magnitude for an upper bound can be estimated from the diffusion constants for the respective species. However, diffusion restrictions within an aggregate could significantly decrease these values. Figure 18

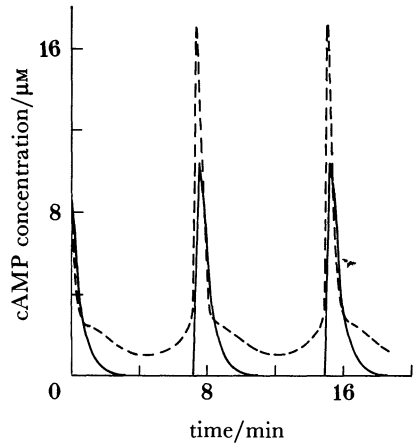

FIGURE 18. The time course of cyclic AMP on a periodic solution when aggregation of the cells into clusters is incorporated. Parameters used are those in table 3, with $V_1 = 0.5$ (as in §4), $\epsilon = 0.9$, $K_{Ca} = 5$, and $K_{CP} = 5$. Solid line: ten times the extracellular cyclic AMP concentration; broken line: intracellular cyclic AMP. The extracellular cyclic AMP shown is the weighted average of the concentrations in the cluster and the exterior compartment, i.e.

$$K_m(\rho\epsilon x_1 + (1-\rho(1+\epsilon))\, x_7)/(1-\rho).$$

One sees that the peak of extracellular cyclic AMP is broadened and decreased compared with the corresponding results for a homogeneous suspension given in figure 12*a*. Here the half-width of the intracellular cyclic AMP peak is less than that of extracellular cyclic AMP, in accordance with the observations of Gerisch & Wick (1975), shown in figure 12.

shows the results of solving (10) with (18) replacing the equations for the external variables and taking $K_{CP} = K_{Ca} = 5$, which is a low value for these constants. All the remaining parameter values are given in table 3 except V_1, which is 0.5.

The principal effects of this change are to shelter some of the secreted cyclic AMP from membrane-bound phosphodiesterase (which is the more active of the two external enzymes) and to shelter this cyclic AMP from membrane-bound cyclic AMP receptors. These have the effect of producing smaller amplitude external cyclic AMP peaks with a larger half-width when compared with results for (10). In fact, with aggregation or incomplete stirring, the half-width for the external cyclic AMP peak can exceed the half-width of the internal cyclic AMP oscillation. This effect may explain why the results given in §4 do not agree with the experimental results of Gerisch *et al.* (1975) regarding the relative half-widths of the internal and external oscillations of cyclic AMP.

The period of the cyclic AMP oscillations in figure 18 is essentially the same as in figure 12, which indicates that there is sufficient calcium in the aggregate to allow adaptation for these parameter values. For other choices of the parameters the period is longer because of the fact that calcium must diffuse into the aggregate from the bulk fluid. In this case a larger amplitude external cyclic AMP oscillation results.

5.2. *Entrainment of excitable cells by pacemakers*

Observations of cells aggregating on agar suggest that only a small fraction of the cells in a population become pacemakers (Raman *et al.* 1976). Although this has not been established for cells in suspension, we now investigate a modification of the basic model given by (10) that allows for two populations of cells with different properties. We assume that the two types of cell differ only in the value of V_1, the constant factor multiplying the adenylate cyclase velocity.

One population is assumed to be relay-competent but not capable of autonomous oscillations, whereas the value of V_1 for the other population is chosen so that a suspension of cells of that type at the same total density would oscillate. The question of interest is what fraction of the total cells must be pacemakers to entrain the entire suspension. To state the governing equations, let the two cell populations be denoted (**1**) and (**2**), and let the corresponding state variables be distinguished by a superscript. Thus $x_2^{(1)}$ and $x_2^{(2)}$ denote the dimensionless internal cyclic AMP concentrations in populations (**1**) and (**2**), respectively, and similarly for x_3 and x_4. Further, let μ denote the fraction of all cells of type (**1**); then $1-\mu$ is the fraction of type (**2**) and the equations are

$$\left.\begin{aligned}
\frac{\mathrm{d}x_1}{\mathrm{d}\tau} &= R_c\left(\frac{\rho}{1-\rho}\right)\Big(\mu[R_H f_2(x_2^{(1)}) + HR_H(R_H x_2^{(1)} - x_1)] - V_{PO}\left(\frac{x_1^\alpha}{1+x_1^\alpha}\right)\\
&\quad + (1-\mu)\,[R_H f_2(x_2^{(2)}) + HR_H(R_H x_2^{(2)} - x_1)] - V_{PE}\left(\frac{x_1}{R_e + x_1}\right)\Big),\\
\frac{\mathrm{d}x_2^{(i)}}{\mathrm{d}\tau} &= V^i(x_1, x_3^{(i)}) + H(x_1 - R_H x_2^{(i)}) - f_2(x_2^{(i)}) - V_{PI}\left(\frac{x_2^{(i)}}{1+x_2^{(i)}}\right),\\
\frac{\mathrm{d}x_3^{(i)}}{\mathrm{d}\tau} &= R_1(x_1)\left(\frac{x_6}{K_F + x_6}\right) - V_{PU}\left(\frac{(x_3^{(i)})^{q_4}}{K_{PU}^{q_4} + (x_3^{(i)})^{q_4}}\right)\\
&\quad + V_S\left(\frac{R_S + K_S x_2^{(i)}}{1 + K_S x_2^{(i)}}\right)(x_4^{(i)} - x_3^{(i)}) - V_{SA}\left(\frac{(x_3^{(i)})^{q_5}}{1 + (x_3^{(i)})^{q_5}}\right),\\
\frac{\mathrm{d}x_4^{(i)}}{\mathrm{d}\tau} &= \left(\frac{R_c}{1-R_c}\right)\left(V_{SA}\left(\frac{(x_3^{(i)})^{q_5}}{1 + (x_3^{(i)})^{q_5}}\right) - V_S\left(\frac{R_S + K_S x_2^{(i)}}{1 + K_S x_2^{(i)}}\right)(x_4^{(i)} - x_3^{(i)})\right),\\
x_6 &= \left(\frac{1}{1-\rho}\right)(\bar{x}_6 - \mu\,[R_c \rho x_3^{(1)} + (1-R_c)\,\rho x_4^{(1)}] - (1-\mu)\,[R_c \rho x_3^{(2)} + (1-R_c)\,\rho x_4^{(2)}]).
\end{aligned}\right\} \quad (19)$$

In the above equations V^i denotes the enzyme velocity function given by (11) with V_1 replaced by V_1^i.

Figure 19 shows the locus of Hopf points for (19) in (μ, V_1^1) space. Parameters except for V_1^i and μ are as given in table 3, and $V_1^{(2)} = 0.13$. As we have seen in §4 for homogeneous suspensions, periodic solutions arise by Hopf bifurcation as V_1 is increased from zero. Thus the hatched region in figure 19, within which the steady state is unstable, delimits the minimal region in parameter space where periodic solutions exist. Consider an initially homogeneous population of relay competent but not autonomous cells, and suppose that a given fraction μ of these cells progress developmentally by an increase in adenylate cyclase velocity (i.e. V_1^1 increases and V_1^2 is fixed). The mixture will begin oscillating periodically if the path in parameter space crosses the lower branch of Hopf points in figure 19. Clearly there is a critical value of μ below which the autonomous subpopulation cannot drive the excitable population periodically. In figure 19 this value is about 0.07, which implies that about 7% of the population must become 'pacemaker competent' before the mixture will oscillate periodically.

5.3. *Time delays in the controlling processes*

In our model all the intermediate steps in the transduction of the external signal and the activation of adenylate cyclase are instantaneous, as is the inhibitory effect of calcium. As we

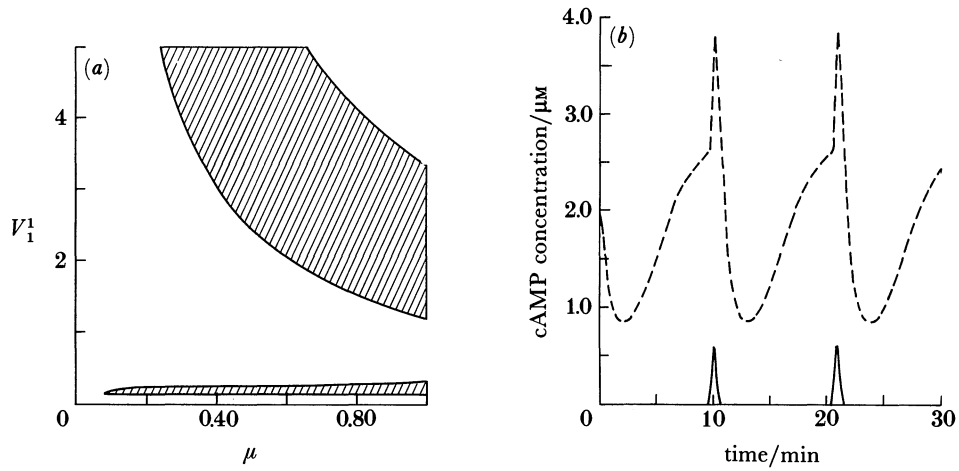

FIGURE 19. The dependence of the solution on the parameters μ and V_1^1. A fraction μ of the population of cells are pacemakers; the remainder are relay competent. (*a*) This diagram shows the loci of Hopf bifurcation points in the (μ, V_1^1) plane. The steady state is unstable in the hatched region. Clearly there is a critical value of the fraction of pacemaker cells μ below which the pacemakers cannot entrain the population. (*b*) The temporal variation of cyclic AMP on the periodic solution for $V_1^1 = 0.14$ and $\mu = 0.1$. The period is within experimental ranges, but the amplitude is low. However, other modifications could be made to increase the amplitude, such as introducing a delay in the action of calcium on adenylate cyclase (see §5.3).

have noted in (I), it is likely that neither of these suppositions is exactly correct. For instance, some processes in the enzyme model may be rather slow, or the receptor and enzyme may not be precoupled, so that receptor–enzyme coupling may slow the transduction of external signal to adenylate cyclase. Similarly, there may be a delay in the transduction of the signal that activates calcium channels in the cell membrane. On the other hand, calcium may not act directly on adenylate cyclase but may act through a chain of intermediate species that includes, for example, calmodulin. In either case there may be a delay in the transduction of the stimulus or in the adaptation process. One way to see how such delays in the control processes might affect the dynamics is to include some time delays in the effect of x_1 and x_3 on the velocity of adenylate cyclase, and in the effect of x_1 on the rate of influx of external calcium.

When time delays are included the models for perfusion and suspension experiments differ from the standard models discussed in §2 only in that the adenylate cyclase velocity term V and the permeability term R_1 now depend on delayed variables. If τ_1 and τ_2 denote the time delay in cyclic AMP and calcium, respectively, then $V(x_1, x_3)$ is replaced by $V(x_{1,\tau_1}, x_{3,\tau_2})$, where $x_{1,\tau_1}(\tau) = x_1(\tau - \tau_1)$ and $x_{3,\tau_2}(\tau) = x_3(\tau - \tau_2)$, and $R_1(x_1)$ is replaced by $R_1(x_{1,\tau_1})$ in (5) and (10).

Let us first discuss delays in the calcium action on adenylate cyclase alone, in which case $\tau_1 = 0$ and $\tau_2 > 0$. Figure 20*a* shows the results of modelling the perfusion experiments with a 6 s delay in calcium. Clearly the general form and amplitude of the secretion rate is unaffected by the delay. The last peak is now a little lower than the third peak, but other parameters in the model could be adjusted slightly to bring that peak up. The effect of a delay in inhibition on the dynamics of suspensions is more pronounced, as is shown in figure 20*b*. The delay in the action of calcium leads to a larger amplitude oscillation in external and internal cyclic AMP because the rise in the inhibition of adenylate cyclase is delayed. The period of the oscillation is also increased because the cells take up more calcium than in the undelayed case, and as a

PHILOSOPHICAL TRANSACTIONS OF THE ROYAL SOCIETY B BIOLOGICAL SCIENCES

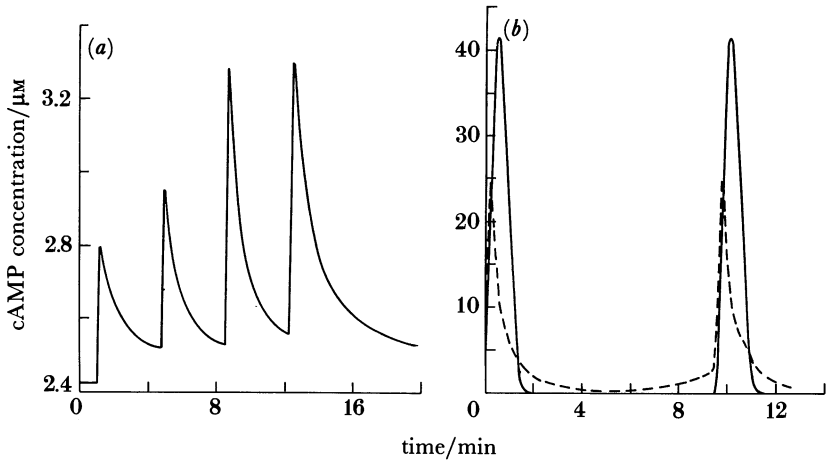

FIGURE 20. The effects of introducing a time delay into the action of calcium on adenylate cyclase. We show the time-course of cyclic AMP for both the perfusion and suspension models in the presence of a 6 s delay. As is to be expected the amplitude of the peak responses is increased because adenylate cyclase remains activated longer. Apart from the delay factors and V_1, all parameters are as in table 3. (*a*) The intracellular cyclic AMP concentration for the perfusion experiment model (see §2) with $V_1 = 0.12$ and a 6 s delay in the action of calcium on adenylate cyclase. The peaks are more rounded and of higher amplitude than those shown in figure 5. This effect is further accentuated by a 30 s delay (not shown here). (*b*) The intracellular and extracellular cyclic AMP concentration for the suspension model (10) with $V_1 = 0.5$ and a 6 s delay in the action of calcium on adenylate cyclase. Although the intracellular concentration is a little high, the results are still in general agreement with experiment (cf. figure 12). Solid line: extracellular cyclic AMP concentration times ten; broken line: intracellular cyclic AMP concentration. Periodic behaviour is seen even with a 30 s delay (not shown).

result, adenylate cyclase is inhibited longer. We have also investigated a 30 s delay in calcium action, and the trends discussed above are also evident with the longer delay. Clearly the presence of a delay does not destroy the general nature of the solutions, and in fact is one mechanism for generating larger amplitude solutions. The period of the oscillations could be controlled by adjusting the rate constants in the calcium system.

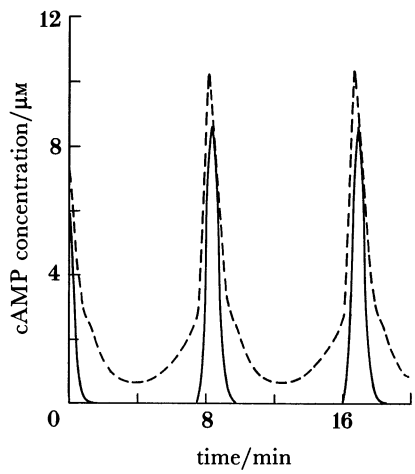

FIGURE 21. The effects of a 6 s delay in the action of extracellular cyclic AMP in activating adenylate cyclase and in opening calcium channels. Parameters are as in table 3 and $V_1 = 0.5$. Solid line: extracellular cyclic AMP concentration times ten; broken line: intracellular cyclic AMP concentration. The amplitude of the oscillations is slightly decreased as compared with figure 12. A still smaller amplitude periodic response is seen with a 30 s delay.

PHILOSOPHICAL TRANSACTIONS OF THE ROYAL SOCIETY B BIOLOGICAL SCIENCES

Finally, we consider the effects of a delay in the action of extracellular cyclic AMP. In this case $\tau_1 > 0$ and $\tau_2 = 0$. In the perfusion experiments the delay will not effect the shape of the response, but will simply translate the response relative to the stimulus. Thus the peak in the secretion rate will lag the onset of stimulation more than in the undelayed case. The effect of a 6 s delay in the activation of the enzyme on the solutions of the model for suspensions is shown in figure 21. The cyclic AMP peaks are lower and the base is somewhat broader compared with those for the corresponding parameters without time delays (cf. figure 12). Even a 30 s delay in the action of extracellular cyclic AMP does not destroy periodicity, which implies that the qualitative features of the model predictions are very robust to time delays in the activation of the enzyme.

6. Conclusion

We have presented a model for the control of cyclic AMP production in *Dictyostelium discoideum*, and have shown that it successfully reproduces most of the experimental results available for perfusion and suspension experiments. This has been achieved by using the same parameters to model both perfusion and suspension experiments, except for the velocity of adenylate cyclase. We have treated this parameter as a variable because experiments suggest that it changes with the developmental age of the cells. Moreover, we have investigated several modifications to the basic model and have shown that they do not alter the general conclusions reached. In particular, we have studied the effects of time delays in the stimulus and adaptation pathways to allow for much longer control pathways than in our basic model. Because the model works well even with considerable delays, it seems likely that we could incorporate more elaborate mechanisms for each control step if these are indicated by experiments.

In addition, we have also shown how to modify the model so as to apply to suspensions that are not homogeneous mixtures of a single cell type, and have shown how the aggregation of cells into small clumps in suspension can change the details of observed cyclic AMP oscillations. It was found that a small fraction of pacemaker cells can entrain a much larger fraction of relay competent cells in suspension. Thus even if only a few cells are autonomous oscillators, as is the case in aggregating fields of cells, still the model predicts that periodic behaviour will exist for appropriate parameter values. Of course, it is possible that a complete model of cellular suspensions must include both multiple populations of cells and aggregation.

As is true in most models of *Dictyostelium*, the activation of adenylate cyclase by extracellular cyclic AMP is an essential step in the mechanism for oscillation in our model. If signal transduction through the membrane is eliminated, oscillations are impossible. Pure cytoplasmic oscillators also exist, in particular those involving calcium-induced release of calcium from internal stores. Although the calcium subsystem cannot oscillate in our model, the possibility of a cytoplasmic oscillator that drives cyclic AMP oscillations should not be dismissed because the experiments of Bumann *et al.* (1986) suggest that an autonomous calcium oscillator may exist (see also Durston 1977).

It will undoubtedly be necessary to modify the postulated network for relay and adaptation as further information on the molecular basis of these processes becomes available. At this stage a reasonable objective is to obtain a model for the cell that adequately reproduces the stimulus–response coupling for external cyclic AMP in *Dictyostelium*. Our model does this for the suspension and perfusion experiments as regards the magnitude and the time-course of the response. With such an input–output model in hand one can address the aggregation problem,

PHILOSOPHICAL TRANSACTIONS OF THE ROYAL SOCIETY B BIOLOGICAL SCIENCES

which requires a model that predicts the observed spatial and temporal distribution of the chemoattractant and the cell density during aggregation. If the stimulus–response model reproduces the observations made in the context of the perfusion and suspension experiments well enough it should be adequate for the aggregation problem, irrespective of the details of the internal dynamics. The model we developed in (II) and herein provides such a description, and our work so far on the aggregation problem shows that we can predict the correct wave speeds and the spiral concentration patterns that are observed in aggregation fields (Othmer & Monk 1988, and unpublished results).

Several other models for cyclic AMP control and synthesis in *Dictyostelium* have appeared in the literature, some of which were discussed in (I). A model based on Monod–Wyman–Changeux concerted transition enzyme kinetics was developed by Goldbeter & Segel (1977). This model was altered slightly and further analysed in Goldbeter & Segel (1980) to explain the transitions in behaviour that are thought to result from developmental changes in enzyme parameters. When applied to suspensions these models predict that ATP oscillates with an appreciable amplitude, which contradicts experimental evidence (see (I) for a detailed discussion of the experimental evidence concerning this model).

Recently, Goldbeter *et al.* have proposed a new type of model. The first version of this model, which is discussed by Goldbeter & Martiel (Goldbeter *et al.* 1984; Martiel & Goldbeter 1984; Goldbeter & Martiel 1985), is based on the supposition that adaptation results from receptor modification, but this model does not incorporate calcium dynamics. Moreover, as we pointed out (Rapp *et al.* 1985*a*), this model has serious defects. For instance, when extracellular cyclic AMP is clamped at zero, as in some of the perfusion experiments, the model does not have a steady state; the level of ATP simply increases monotonically without bound. Also, the model cannot reproduce the experimentally observed response to a series of step increases in the external cyclic AMP concentration (cf. figure 4 herein). Related receptor modification schemes have been described (Knox *et al.* 1986; Segel *et al.* 1986). The most recent version of the Goldbeter–Martiel model is presented in Martiel & Goldbeter (1987) and incorporates the receptor modification scheme of Knox *et al.* (1986) and Segel *et al.* (1986). This version does not have the defects of the previous version, and appears to explain many aspects of adaptation and periodicity. However, it is still not clear that the model can show the correct adaptive behaviour to an increasing staircase of stimuli (as shown in figure 4 for our model).

Models involving receptor modification are motivated by the experimental observations of Theibert *et al.* (1984), Klein *et al.* (1985*a*, *b*) and Devreotes & Sherring (1985). These investigators have found that external cyclic AMP induces a reversible change in the electrophoretic mobility of the cyclic AMP receptor. This reversible change is found to correlate with adaptation and deadaptation, which suggests that receptor modification may be the biochemical mechanism of adaptation in *Dictyostelium*. Devreotes & Sherring (1985) suggest that cyclic-AMP-induced phosphorylation of the receptor leads to the observed behaviour, and they suggest a molecular model to explain their findings. Our model also involves modification of the receptor–enzyme complex via interaction with calcium. Whether receptor modification is induced by interactions within the receptor system, as in the models of Goldbeter *et al.*, or reactions subsequent to the binding of cyclic AMP to the receptor, as in our model, is not yet known.

There is indirect evidence that calcium inhibits adenylate cyclase in *Dictyostelium*, and that calcium is responsible for adaptation. Caffeine is known to inhibit activation of adenylate

cyclase reversibly (Theibert & Devreotes 1983; Brenner & Thomas 1984), as is shown in figure 22*a*. Brenner & Thomas (1984) present results that suggest that caffeine acts by increasing the level of cytoplasmic calcium in *Dictyostelium*. Moreover, experiments using a calcium ionophore yield similar results to experiments with caffeine, as is shown in figure 22*b*. This result suggests that cytoplasmic calcium levels control inhibition of adenylate cyclase. The results of Brenner & Thomas (1984) also suggest that release of calcium from internal stores may be important (cf. also Europe-Finner & Newell (1985)).

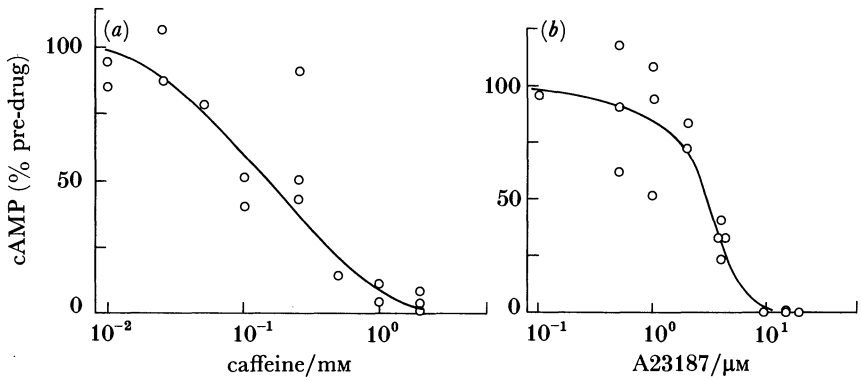

FIGURE 22. (*a*) A reproduction of figure 3 from Brenner & Thomas (1984). This graph shows the ratio of the response (total amount of labelled cyclic AMP secreted over a fixed time) to 30 nM cyclic AMP pulses with caffeine and without caffeine. Cells are in suspension and exhibit light-scattering oscillations. (*b*) A reproduction of figure 6 from Brenner & Thomas (1984). This graph shows the ratio of the response (total amount of labelled cyclic AMP secreted over a fixed time) to 100 nM cyclic AMP pulses with ionophore and without ionophore. As in (*a*), cells are in suspension and exhibit light-scattering oscillations.

The model presented in this paper only concerns the relay response. However, cyclic AMP stimuli also trigger a chemotactic response (see Introduction). To model the cellular response more completely we would have to incorporate cyclic GMP and perhaps other species (Van Haastert & Konijn 1983). The inclusion of cyclic GMP in the model might make the model applicable to other systems, because although there are certainly cell specific variations, second messenger control systems similar to that in *Dictyostelium* are present in a wide range of systems. In fact, calcium cyclic nucleotide mediation of stimulus–response adaptation appears to be an evolutionarily conserved strategy. Thus the range of applicability of this investigation may well extend beyond *Dictyostelium*.

Conversations with Peter Devreotes, Julian Gross and Peter Newell at various stages were helpful in the development of the model and the interpretation of experimental results. This research was done in part while P.B.M. was visiting the University of Maryland, Baltimore County. P.B.M. was supported in part by a grant from the NSF. H.G.O. was supported in part by NIH grant GM 29123.

PHILOSOPHICAL TRANSACTIONS OF THE ROYAL SOCIETY B BIOLOGICAL SCIENCES

Appendix 1. Parameters in the external compartment

In this section we derive the non-dimensional parameters used in the external compartment.

A.1. K_m, K_e *and* V_c

A value of $K_m = 0.5$ μM is reported in Malchow *et al.* (1975), and a value of $K_e = 1.3$ mM is reported in Kessin *et al.* (1979) and Chassy (1972) for the inhibited enzyme. We use $K_e = 1.0$ mM. This gives a value for R_e of 2000, which is close to the measured value of 2600. In Rapp *et al.* (1985*b*), we have previously calculated a value of 700 μm^3 for the volume of a single cell.

A.2. *Velocity of membrane-bound phosphodiesterase*

Roos *et al.* (1977) give a value of 1.67×10^6 molecules per cell per second for this enzyme. From table 2, we find that

$$V_{PO} = \frac{k_0'(\mathrm{m}PDE_0)\, A_c}{k_5(\mathrm{i}PDE_0)\, V_c\, K_m}$$

and $k_0'(\mathrm{m}PDE_0)\, A_c$ = velocity of enzyme in micromoles per minute per cell.

Using the value for $k_5(\mathrm{i}PDE_0)$ from table 3 we can then compute that V_{PO} should be approximately 230. This parameter varies with the developmental age of the cell (see §4). We use the value $V_{PO} = 100$, but have investigated varying V_{PO} from that value (see §4).

A.3. *Velocity of free phosphodiesterase*

An enzyme velocity of 3×10^7 molecules per cell per second has been measured by Yamasaki & Hayashi (1982). From table 2 we see that

$$V_{PE} = \frac{k_6'(\mathrm{e}PDE_0)}{k_5(\mathrm{i}PDE_0)\, V_c\, K_m}$$

and $k_6'(\mathrm{e}PDE_0)$ = velocity of enzymes in micromoles per minute per cell.

Hence we find that V_{PE} is approximately 5000, which is the value we use.

A.4. ρ

From table 2,

$$\rho = \frac{N(V_c + V_s)}{N(V_c + V_s) + V_0}.$$

From Rapp *et al.* (1985*b*), $V_c + V_s = 7 \times 10^{-10}$ cm^3 and a typical cell density for experiments is

$$\frac{N}{V_0 + N(V_c + V_s)} = 2 \times 10^8 \text{ cells per cubic centimetre.}$$

From these one finds that $\rho = 0.14$. We use $\rho = 0.1$ as the standard value for the simulations of suspension experiments.

References

Abe, K. & Yanagisawa, K. 1983 A new class of rapidly developing mutants in *Dictyostelium discoideum*: implications for cyclic AMP metabolism and cell differentiation. *Devl Biol.* **95**, 200–210.

Bonner, J. 1967 *The cellular slime molds*. Princeton University Press.

Brenner, M. 1978 Cyclic AMP levels and turnover during development in the cellular slime mold *Dictyostelium discoideum*. *Proc. natn. Acad. Sci. U.S.A.* **64**, 210–223.

PHILOSOPHICAL TRANSACTIONS OF THE ROYAL SOCIETY B BIOLOGICAL SCIENCES

Brenner, M. & Thomas, S. 1984 Caffeine blocks activation of cyclic AMP synthesis in *Dictyostelium discoideum*. *Devl Biol.* **101**, 136–146.

Bumann, J., Wurster, B. & Malchow, D. 1984 Attractant-induced changes and oscillations of the extracellular Ca^{++} concentrations in suspensions of differentiating *Dictyostelium* cells. *J. Cell Biol.* **98**, 173–178.

Bumann, J., Malchow, D. & Wurster, B. 1986 Oscillations of Ca^{++} concentration during the cell differentiation of *Dictyostelium discoideum*. *Differentiation* **31**, 85–91.

Chassy, B. 1972 Cyclic nucleotide phosphodiesterase in *Dictyostelium discoideum*. Interconversisn of two enzyme types. *Science, Wash.* **175**, 1016–1018.

Devreotes, P. & Sherring, J. 1985 Kinetics and concentration dependence of reversible cAMP-induced modification of the surface cAMP receptor in *Dictyostelium*. *J. biol. Chem.* **260**, 6378–6384.

Devreotes, P. & Steck, T. 1979 Cyclic 3′,5′ AMP relay in *Dictyostelium discoideum*. II. Requirements for the initiation and termination of the response. *J. Cell Biol.* **80**, 300–309.

Devreotes, P., Derstine, P, & Steck, T. 1979 Cyclic 3′,5′ AMP relay in *Dictyostelium discoideum*. I. A technique to monitor responses to controlled stimuli. *J. Cell Biol.* **80**, 291–299.

Dinauer, M., MacKay, S. & Devreotes, P. 1980*a* Cyclic 3′,5′ AMP relay in *Dictyostelium discoideum*. III. The relationship of cAMP synthesis and secretion during the cAMP signaling response. *J. Cell Biol.* **86**, 537–544.

Dinauer, M., Steck, T. & Devreotes, P. 1980*b* Cyclic 3′,5′ AMP relay in *Dictyostelium discoideum*. IV. Recovery of the cAMP signaling response after adaptation to cAMP. *J. Cell Biol.* **86**, 545–553.

Dinauer, M., Steck, T. & Devreotes, P. 1980*c* Cyclic 3′,5′ AMP relay in *Dictyostelium discoideum*. V. Adaptation of the cAMP signaling response during cAMP stimulation. *J. Cell Biol.* **86**, 554–561.

Doedel, E. & Kernevez, J. 1986 Software for continuation problems in ordinary differential equations with applications. Technical report, California Institute of Technology.

Durston, A. 1977 The control of morphogenesis in *Dictyostelium discoideum*. In *Eucaryotic microbes as model developmental systems* (ed. P. Horgan & D. O'Day), pp. 294–321. New York: Marcel Dekker.

Europe-Finner, G. & Newell, P. 1985 Calcium transport in the cellular slime mold *Dictyostelium discoideum*. *FEBS Lett.* **186**, 70–74.

Gerisch, G. 1968 Cell aggregation and differentiation in *Dictyostelium*. *Curr. Top. devl Biol.* **3**, 157–197.

Gerisch, G. & Hess, B. 1974 Cyclic-AMP-controlled oscillations in suspended *Dictyostelium* cells: their relation to morphogenetic cell interactions. *Proc. natn. Acad. Sci. U.S.A.* **71**, 2118–2122.

Gerisch, G. & Wick, U. 1975 Intracellular oscillations and release of cyclic AMP from *Dictyostelium* cells. *Biochem. biophys. Res. Commun.* **65**, 364–370.

Gerisch, G., Hulser, D., Malchow, D. & Wick, U. 1975 Cell communication by periodic cyclic-AMP pulses. *Phil. Trans. R. Soc. Lond.* B **272**, 181–192.

Gerisch, G., Malchow, D., Roos, W. & Wick, U. 1979 Oscillations of cyclic nucleotide concentrations in relation to the excitability of *Dictyostelium* cells. *J. exp. Biol.* **81**, 33–47.

Gingle, A. & Robertson, A. 1976 The development of the relaying competence in *Dictyostelium discoideum*. *J. Cell Sci.* **20**, 21–27.

Goldbeter, A. & Martiel, J. 1985 Biorhythmicity in a model for the cyclic AMP signalling system of the slime mold *Dictyostelium discoideum*. *FEBS Lett.* **191**, 149–153.

Goldbeter, A. & Segel, L. 1977 Unified mechanism for relay and oscillation of cyclic AMP in *Dictyostelium discoideum*. *Proc. natn. Acad. Sci. U.S.A.* **74**, 1543–1547.

Goldbeter, A. & Segel, L. 1980 Control of developmental transitions in the cyclic AMP signaling system of *Dictyostelium discoideum*. *Differentiation* **17**, 127–135.

Goldbeter, A., Martiel, J. & Decroly, O. 1984 From excitability and oscillations to birhythmicity and chaos in biochemical systems. In *Dynamics of biochemical systems* (ed. R. J. Cornish-Bowden & A. Cornish-Bowden), pp. 173–212. New York: Plenum Press.

Gottmann, K. & Weijer, C. 1986 In situ measurements of external pH and optical density oscillations in *Dictyostelium discoideum* aggregates. *J. Cell Biol.* **102**, 1623–1629.

Kessin, R., Orlow, S., Shapiro, R. & Franke, J. 1979 Binding of inhibitor alters kinetic and physical properties of extracellular cyclic AMP phosphodiesterase from *Dictyostelium discoideum*. *Proc. natn. Acad. Sci. U.S.A.* **76**, 5450–5454.

Klein, C. 1976 Adenylate cyclase activity in *Dictyostelium discoideum* amoebae and its changes during differentiation. *FEBS Lett.* **68**, 125–128.

Klein, C. & Darmon, M. 1977 Effect of cyclic AMP pulses on adenylate cyclase and the phosphodiesterase inhibitor of *D. discoideum*. *Nature, Lond.* **268**, 76–78.

Klein, C., Lubs-Haukeness, J. & Simons, S. 1985*a* cAMP induces a rapid and reversible modification of the chemotactic receptor in *Dictyostelium discoideum*. *J. Cell Biol.* **100**, 715–720.

Klein, P., Theibert, A. Fontana, D. & Devreotes, P. 1985*b* Identification and cyclic AMP-induced modification of the cyclic AMP receptor in *Dictyostelium discoideum*. *J. biol. Chem.* **260**, 1757–1764.

Knox, B., Devreotes, P., Goldbeter, A. & Segel, L. 1986 A molecular mechanism for sensory adaptation based on ligand-induced receptor modification. *Proc. natn. Acad. Sci. U.S.A.* **83**, 2345–2349.

PHILOSOPHICAL TRANSACTIONS OF THE ROYAL SOCIETY B BIOLOGICAL SCIENCES

Loomis, W. 1979 Biochemistry of aggregation in *Dictyostelium*: a review. *Devl Biol.* **70**, 1–12.
Malchow, D., Fuchila, J. & Nanjundiah, V. 1975 A plausible role for a membrane bound cyclic AMP phosphodiesterase in cellular slime mold chemotaxis. *Biochim. biophys. Acta* **385**, 421–428.
Malchow, D., Nanjundiah, V., Wurster, B., Eckstein, F. & Gerisch, G. 1978 Cyclic AMP-induced pH changes in *Dictyostelium discoideum* and their control by calcium. *Biochim. biophys. Acta* **538**, 473–480.
Malchow, D., Bohme, R. & Gras, U. 1982 On the role of calcium in chemotaxis and oscillations of *Dictyostelium* cells. *Biophys. struct. Mech.* **9**, 131–136.
Martiel, J. & Goldbeter, A. 1984 Oscillations and relay of cAMP signals in *Dictyostelium discoideum*: analysis of a model based on the modification of the cAMP receptors. *C.r. Acad. Sci., Paris* C **298**, 549–552.
Martiel, J. & Goldbeter, A. 1987 A model based on receptor desensitization for cyclic AMP signalling in *Dictyostelium* cells. *Biophys. J.* **52**, 807–828.
Newell, P. C. 1986 The role of actin polymerization in amoebal chemotaxis. *Bioessays* **5**, 202–212.
Othmer, H. 1976 Temporal oscillations in chemically-reacting systems. In *Proceedings of the IEEE International Conference on Cybernetics and Society*, pp. 314–320.
Othmer, H. & Monk, P. 1988 Concentration waves in aggregation fields of a cellular slime mold. In *Biomathematics and related computational problems* (ed. L. M. Ricciardi), pp. 381–398. Dordrecht: Kluwer Academic Publishers.
Othmer, H., Monk, P. & Rapp, P. 1985 A model for signal relay and adaptation in *Dictyostelium discoideum*. Part II. Analytical and numerical results. *Mathl Biosci.* **77**, 77–139.
Pannbacker, R. & Bravard, L. 1972 Phosphodiesterase in *Dictyostelium discoideum* and the chemotactic response to cyclic adenosine monophosphate. *Science, Wash.* **175**, 1014–1015.
Pate, E., Elwood, D. & Othmer, H. 1989 mPDE dramatically affects cAMP levels near aggregating *D. dictyostelium* cells. (In preparation.)
Raman, R., Hashimoto, Y., Cohen, M. & Robertson, A. 1976 Differentiation for aggregation in the cellular slime molds: the emergence of autonomously signalling cells in *Dictyostelium discoideum*. *J. Cell Sci.* **21**, 243–259.
Rapp, P., Monk, P. & Othmer, H. 1985*a* A model for signal relay and adaptation in *Dictyostelium discoideum*. Part I. Biological processes and the model network. *Mathl Biosci.* **77**, 35–78.
Rapp, P., Monk, P. & Othmer, H. 1985*b* *Quantitative estimates of kinetic parameters in the calcium cyclic nucleotide network in Dictyostelium discoideum*. Technical Report, Department of Physiology and Biochemistry, Medical College of Pennsylvania, Philadelphia.
Roos, W., Scheidegger, C. & Gerisch, G. 1977 Adenylate cyclase activity oscillations as signals for cell aggregation in *Dictyostelium discoideum*. *Nature, Lond.* **266**, 259–260.
Segel, L., Goldbeter, A., Devreotes, P. & Knox, B. 1986 A mechanism for sensory adaptation based on receptor modification. *J. theor. Biol.* **120**, 151–179.
Theibert, A. & Devreotes, P. 1983 Cyclic 3′,5′-AMP relay in *Dictyostelium discoideum*: adaptation is independent of activation of adenylate cyclase. *J. Cell Biol.* **97**, 173–177.
Theibert, A., Klein, P. & Devreotes, P. 1984 Specific photoaffinity labeling of the cAMP surface receptor in *Dictyostelium discoideum*. *J. biol. Chem.* **259**, 12318–12321.
Van Haastert, P. & Konijn, T. 1983 Signal transduction in the cellular slime molds. *Molec. cell. Endocr.* **26**, 1–17.
Weijer, C., McDonald, S. & Durston, A. 1984 A frequency difference in optical density oscillations of early *Dictyostelium discoideum* density classes and its implication for development. *Differentiation* **28**, 9–12.
Wurster, B. & Butz, U. 1983 A study on sensing and adaptation in *Dictyostelium discoideum* guanosine 3′,5′-phosphate accumulation and light-scattering responses. *J. Cell Biol.* **96**, 1566–1570.
Yamasaki, F. & Hayashi, H. 1982 Comparison of properties of the cellular and extracellular phosphodiesterase induced by cyclic adenosine 3′,5′-monophosphate in *Dictyostelium discoideum*. *J. Biochem.* **91**, 981–988.

PHILOSOPHICAL TRANSACTIONS OF THE ROYAL SOCIETY B BIOLOGICAL SCIENCES